ADVANCED MATERIALS TECHNOLOGIES
www.advmattechnol.de

Triboelectric Nanogenerators with Machine Learning for Internet of Things

Jiayi Yang, Keke Hong, Yijun Hao, Xiaopeng Zhu, Yong Qin, Wei Su, Hongke Zhang, Chuguo Zhang, Zhong Lin Wang,* and Xiuhan Li**

The development of the Internet of Things (IoT) indicates that humankind has entered a new intelligent era of the "Internet of Everything". Thanks to the characteristics of low-cost, diverse structure, and high energy conversion efficiency, the self-powered sensing systems, which are based on the Triboelectric Nanogenerator (TENG), demonstrate great potential in the field of IoT. In order to solve the challenges of TENG in sensing signal processing, such as signal noise and nonlinear relations, Machine Learning (ML), which is an efficient and mature data processing tool, is widely applied for efficiently processing the large and complex output signal data generated by TENG intelligent sensing system. This review summarizes and analyzes the adaptation of different algorithms in TENG and their advantages and disadvantages at the beginning, which provides a reference for the selection of algorithms for TENG. More importantly, the application of TENG is introduced in multiple scenarios, including health monitoring, fault detection, and human-computer interaction. Finally, the limitations and development trend of the integration of TENG and ML are proposed by classification to promote the future development of the intelligent IoT era.

1. Introduction

The Internet of Things (IoT) has become an important driving force for the new round of global technological revolution and industrial transformation.[1–3] By integrating with new manufacturing technologies, such as new energy and new materials to promote the application of new information technologies (5th generation mobile communication technology, narrowband IoT, cloud computing, big data, artificial intelligence, and blockchain) into various fields, caused great changes in the global industrial structure.[4–6] As the popularity of IoT applications, trillions of new devices with different application requirements are connected to the network, which makes the collection and analysis of big data based on widely distributed wireless sensor networks become increasingly important in information development. The demand for power consumption in wireless sensor networks is also increasing with the development of the IoT.[7] Although the power consumption of the single sensor is low, the power consumption of trillions of sensing units will reach an astonishing height, making the power consumption of the IoT extremely high. In addition, traditional sensing units, such as pressure sensors, temperature sensors, gas sensors, and humidity sensors, face inherent limitations such as frequent charging, harsh environmental impacts, maintenance costs, equipment life, and waste recycling.[8–13] Therefore, the total energy expenditure of wireless sensor networks, as well as the distributed energy requirements and inherent limitations of sensors, have become key and urgent issues that need to be solved by IoT technology. To address this critical problem, the development of distributed self-powered sensing units without external power supply is currently an effective and sustainable solution.

As an emerging technology for mechanical energy harvesting and self-powered sensing, triboelectric nanogenerator (TENG) shows great potential to break through relevant restrictions. In 2012, corresponding researchers developed the TENG for converting distributed, disordered, low-frequency mechanical energy into electrical energy.[14] TENG has attracted wide attention due to its low price, diverse structure, light weight, and environmental and ecological friendliness.[15–17] In addition, since it can effectively record various environmental information without the supply of external power, such as tactile, pressure and vibration, TENG can be used as a self-powered sensor as well.[18–21] In recent years, to promote the application of TENG with IoT, researchers have greatly improved the output characteristic of TENG through triboelectric material modification,[22–25] device structure optimization,[26–30] and polarization charge injection.[31–33] However, there are still shortcomings in TENG signal processing. Friction between nanomaterials generates noise, which can interfere with signal processing and transmission, thus degrading the performance of the

J. Yang, K. Hong, Y. Hao, X. Zhu, Y. Qin, W. Su, H. Zhang, C. Zhang, X. Li
School of Electronic and Information Engineering
Beijing Jiaotong University
Beijing 100044, P. R. China
E-mail: cgzhang@bjtu.edu.cn; lixiuhan@bjtu.edu.cn

Z. L. Wang
Beijing Institute of Nanoenergy and Nanosystems
Chinese Academy of Sciences
Beijing 100083, China
E-mail: zhong.wang@mse.gatech.edu

The ORCID identification number(s) for the author(s) of this article can be found under https://doi.org/10.1002/admt.202400554

DOI: 10.1002/admt.202400554

system and leading to signal quality degradation.[34–36] Besides, the output performance of the TENG is finite, which will lead to signal attenuation, affecting the signal processing and analysis ability.[37–39] Moreover, integrating TENG with conventional signal processors to obtain the signal processing also remains a critical issue.[40–45] In TENG system, signal processing is a critical task, particularly in complex application scenarios where signal characteristics are highly variable, which directly affects the performance and practicability of the system. It is difficult to accurately extract the appropriate features of the target by manual methods alone due to the high variability and noise level of the TENG output signal, and traditional signal processing methods often fail to meet these challenges. The machine learning (ML) technology can effectively analyze the TENG output signal and suppress the noise, improving the accuracy, robustness, and efficiency of signal processing.[46–55] In addition, ML can also be used to optimize the signal processing circuit, simplify the processing flow, and effectively reduce the TENG signal processing time and complexity.[56–60] Despite this, research on integrating TENG technology with ML is still in its early stages, and there is a noticeable lack of comprehensive reviews in this interdisciplinary area. This gap indicates a need for in-depth exploration of the theoretical and practical aspects of combining ML with TENG, to realize its potential across various application scenarios.

In this work, we comprehensively elaborate the latest progress of the combination of TENG and ML. The detailed work process of ML is first introduced, and common ML algorithms are listed. In addition, we present the latest research of TENG based on different algorithms. The advantages and disadvantages of different algorithms also are compared, and the algorithms suitable for different TENG are introduced step by step. Subsequently, we divide TENG into four main areas according to the application, and conduct a review, summary, and comparative analysis of the existing excellent work. Meanwhile, we discuss the current application limitations of ML in the field of TENG, explore the solutions, and give relevant suggestions for reference. Finally, the application prospect of the integration of TENG with ML in the future IoT tide is also prospected at last. Thus, we sincerely wish the review can significantly expedite the rapid development of the TENG-based self-powered IoT technology and provide some different research ideas for researchers who have just entered the related research field (**Figure 1**).

2. Working Mechanism of TENG

As two different materials are in contact with each other, their surfaces generate positive and negative charges owing to the contact electrification. When the two materials are separated due to mechanical forces, the positive and negative charges generated by contact electrification are also separated. The charge separation correspondingly creates an induced potential difference between the upper and lower electrodes, which drives electrons to flow between the two electrodes through an external circuit. There are four basic working modes: Vertical Contact-separation Mode,[61–63] Horizontal Sliding Mode,[64–66] Single Electrode Mode,[67–69] Independent Layer Mode,[70–72] as shown in **Figure 2**.

2.1. Vertical Contact-Separation Mode

The structure is that two different dielectric films are in close contact, and electrodes are attached to the back of them. Due to triboelectrification, the inner surfaces of the two materials produce electrostatic charges with equal density and opposite polarity, and an electric potential difference will be generated as the two surfaces are separated. If the two electrodes are connected by an external circuit, electrons will flow from one electrode to the other for balancing the potential difference. As the triboelectric materials come close to each other again, electrons flow back to the original electrode for balancing the potential difference. Common structures of this working mode include spacer structure, arch structure and spring structure, which are widely used in various application scenarios, such as vibration energy collection, acoustic wave collection.[73–75]

2.2. Horizontal Sliding Mode

As two objects are in close contact, they will be positively and negatively charged on the contact surface due to their different electronegativity. As the upper material begins to slide, the contact area between the materials will decrease. In order to balance the potential difference in the uncontacted part, electrons in the upper and lower electrodes flow from the external circuit. When the top material slides back, the positive and negative charges on the surface of the material re-establish the balance relationship, so that the excess charge in the electrode will flow back to the original electrode. Common structures include planar sliding structure, disk structure, and tubular structure, which are widely used in various scenarios, such as displacement sensing and wind energy collection.[76–78]

2.3. Single-Electrode Mode

This working mode has the same contact electrification process as the above two working modes, while the difference is that it only requires one electrode to be connected to one of the TENG electrification surfaces, and the ground is assumed to be the other electrode. Therefore, the other generating surface of the TENG can move freely without the limitation of electrodes, making it widely used in various scenarios, such as tactile sensors, liquid energy collection/detection, and human motion sensors.[79–82]

2.4. Independent Layer Mode

After a moving object is charged by rubbing against other objects, the charge can remain on the surface of the object for a long time. When a pair of symmetric electrodes is placed under a dielectric layer, the independent layer movement between the two electrodes creates an uneven charge distribution, and electrons flow between electrodes for balancing the potential difference. This mode is widely used in ocean energy collection, machine bearing detection.[83–85]

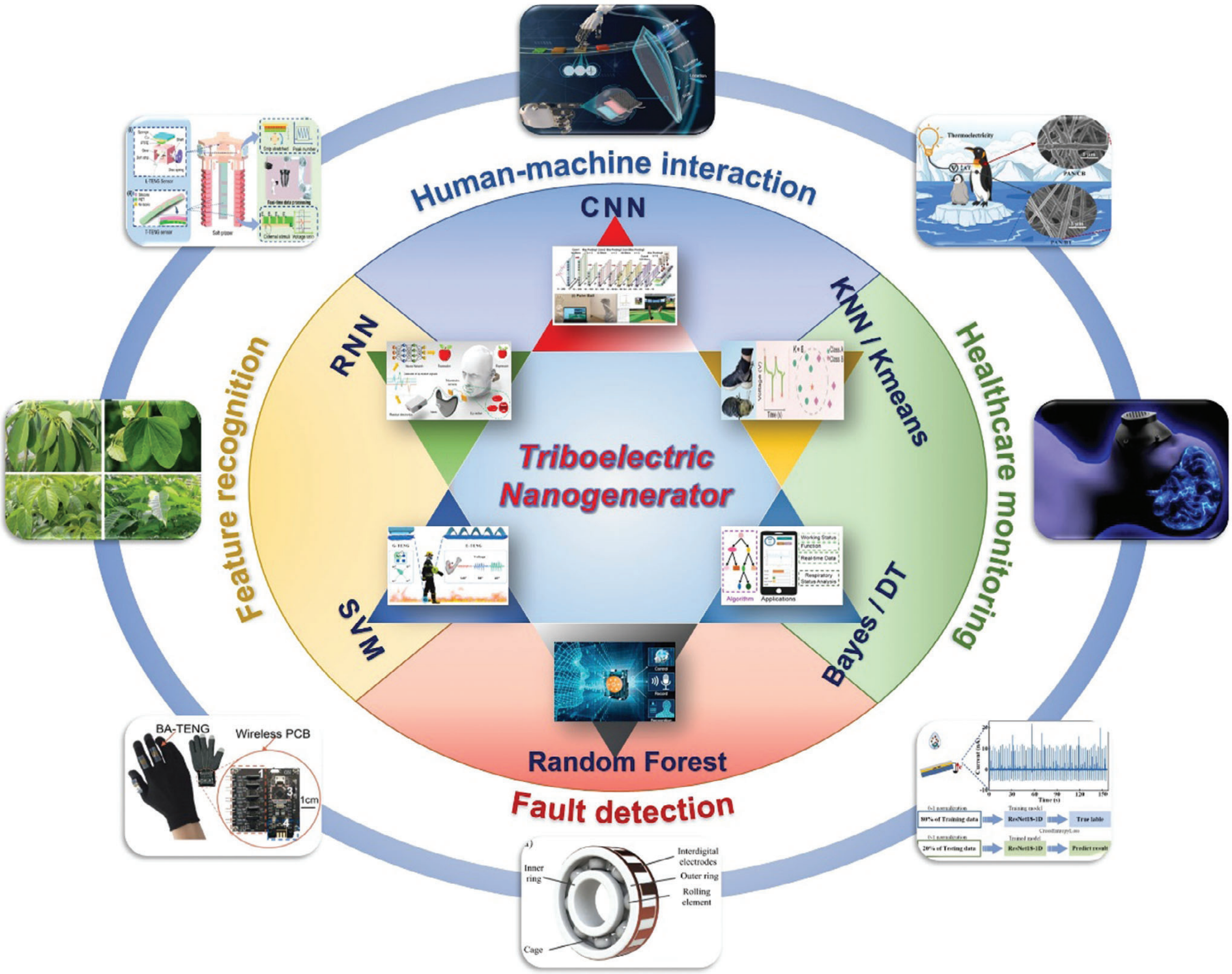

Figure 1. The multi-scenario application of TENG based on different algorithms: The inner layer describes the common algorithms (Naive Bayes, Decision Tree, Random Forest, K-Nearest Neighbor, K-means, Support Vector Machine, Convolutional Neural Network, Recurrent Neural Network) of TENG.[97,100,103,110,120,125] The outer layer describes the application (Healthcare monitoring, Fault detection, Human-machine interaction, Feature recognition) of TENG combining with ML.[99,104,109,134,138,157,122,166] Reproduced with permission.[97,104] Copyright 2023, 2022, MDPI. Reproduced with permission.[100] Copyright 2023, American Chemical Society. Reproduced with permission.[103] Copyright 2022, Springer. Reproduced with permission.[99,109,110,134,138,157] Copyright 2022, 2021, 2021, 2022, 2022, 2020, Elsevier. Reproduced with permission.[120,122] Copyright 2020, 2022, Wiley-VCH. Reproduced with permission.[125,166] Copyright 2022, 2020, Springer Nature.

3. Working Mechanism of Machine Learning

ML is an important branch in the field of artificial intelligence and it mainly includes the following state: i) takes a large amount of data as training samples; ii) extracts key rules from the data through training and optimization; iii) builds relevant models; iv) realizes prediction and decision-making functions. ML algorithms are divided into supervised and unsupervised learning.[86–88] Supervised learning is a method of training the model through labeled data. In supervised learning, the training data is divided into two parts: input and output. By learning the relationship between input and output, a model can be built for predicting the output. Unsupervised learning is a way of learning without labeled data. In unsupervised learning, there are only input data and no corresponding output labels. The algorithm finds the pattern and structure by analyzing and clustering the data. Therefore, ML can efficiently process various types of data produced by TENG, and train data to build models for making predictions or decisions, thereby optimizing the complexity of the signal processing part of TENG sensing system in different application scenarios. **Figure 3** shows the main workflow of ML and the evolution of common algorithm models.

ML covers a variety of algorithms and each algorithm has different characteristics and applicable scenarios. Linear regression is to find the best fitting line for prediction by fitting the linear function of data points.[89] Logistic regression is used to represent probabilities by mapping the output of a linear function to a range of [0,1], and is often used for binary classification problems.[90] Decision Tree (DT) constructs a tree structure, which can divide target data by the value of the feature and finally gets a decision

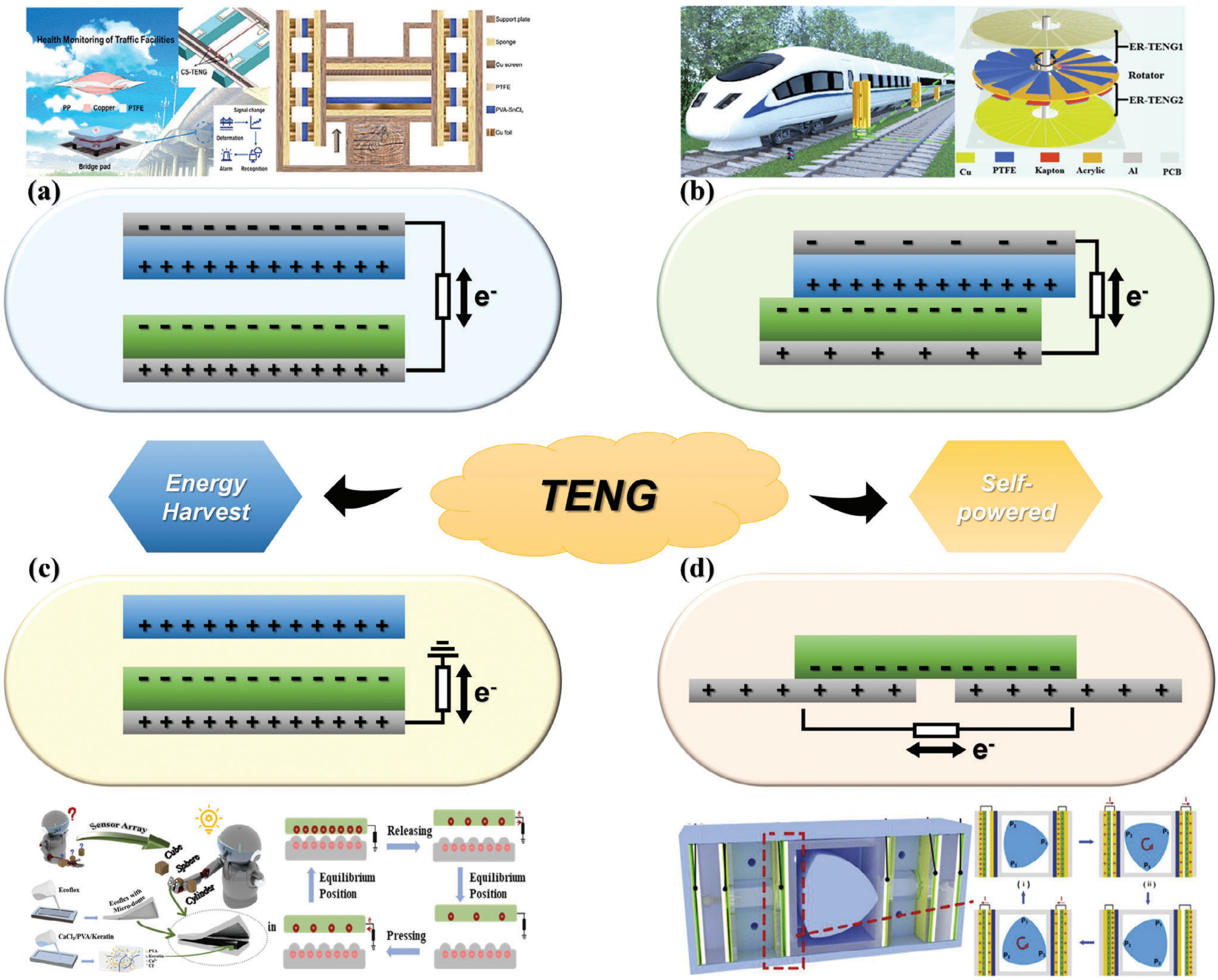

Figure 2. The working mechanism of TENG under different modes and its working scenarios: Vertical Contact-separation Mode,[63] Horizontal Sliding Mode,[66] Single Electrode Mode,[69] and Independent Layer Mode.[72]

path. This way is suitable for processing data with discrete and continuous characteristics.[91] Random Forest (RF) is an ensemble learning algorithm, which is suitable for classification and regression problems. It makes predictions by integrating multiple DTs, and the results of each DT vote to determine the final prediction result. RF algorithm has good generalization ability and robustness, which is suitable for processing high-dimensional features.[92] K-nearest neighbor (KNN) algorithm is an instance-based learning algorithm, which calculates the distance metric to classify new samples, and is suitable for small-scale data and multi-class problems.[93] K-means, one of the most common clustering algorithms, discovers patterns and structures between data by grouping similar data points.[94] Support vector machine (SVM) is suitable for binary classification and multi-classification problems. It separates different classes of samples by searching the best hyperplane. SVM algorithm performs well in high dimensional data and nonlinear problems.[95] Neural network (NN) mimics the biological nervous system and is suitable for a variety of complex tasks. It consists of multiple neurons and hierarchies that learn weights and activation functions to achieve predictive ability (**Table 1**).[96]

ML trains data to build models to make predictions or decisions, its workflow consists of several key steps:

i. Data collection and preprocessing: It is necessary to collect data before ML, which is based on all algorithms needed to explore rules and build models from the data. The output data of TENG with different materials, structures, and application scenarios are different, which is distinct from the conventional ML field that can collect data from the established database. It is necessary for TENG to collect a large amount of data and ensure its quality and integrity for ML. The raw data may have problems of missing values, outliers, or duplicate values. Before feature extraction, the data needs to be preprocessed. Common preprocessing methods include data cleaning, missing value filling, and outlier processing. In addition, if the TENG output is multidimensional signal and the output data is large, Principal Component Analysis

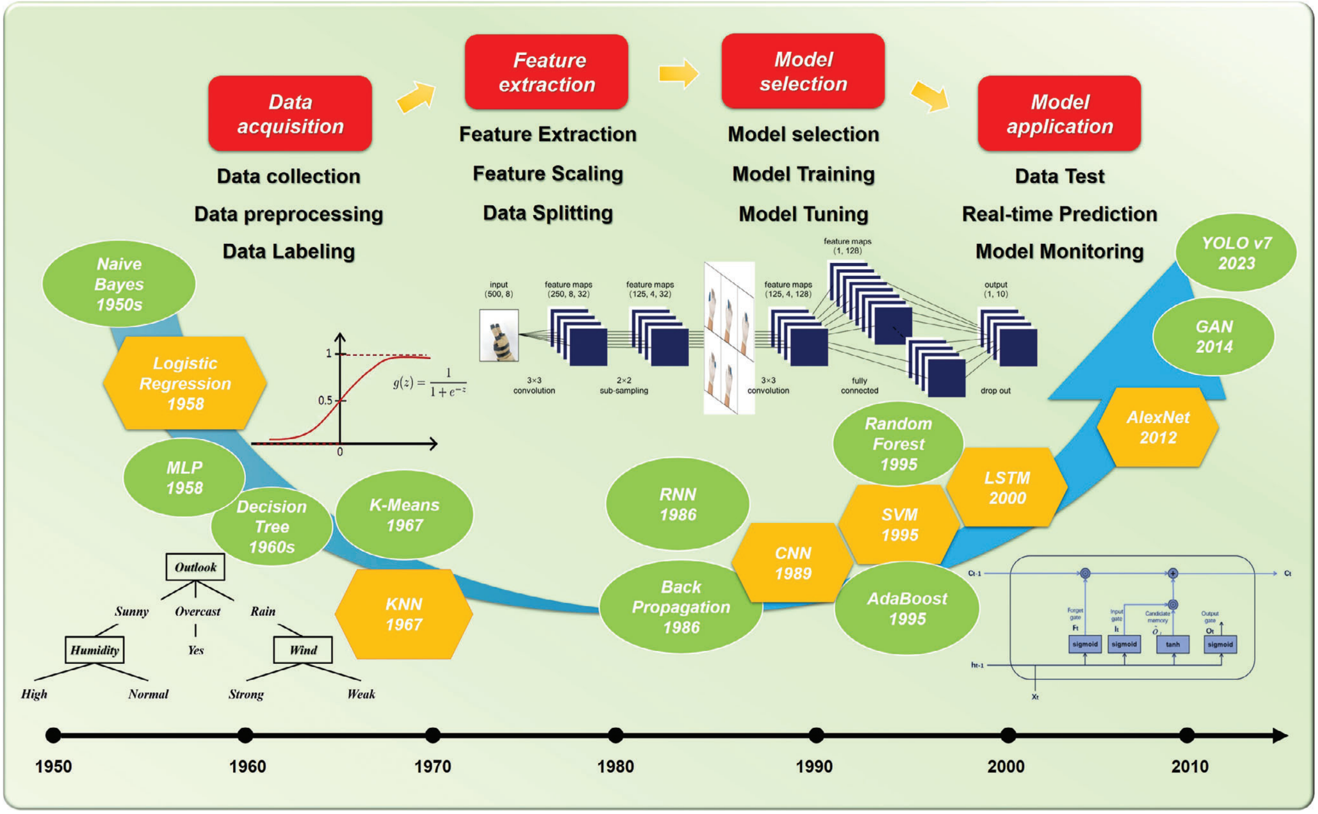

Figure 3. The workflow of ML (Data collection and preprocessing, Feature extraction, Model selection and optimization, Model deployment and application) and the review of historical development.[89–96]

(PCA) can be selected for data dimensionality reduction to improve data processing speed and accuracy of ML. Excellent data preprocessing can improve data quality and enable models to learn from data better, thus optimizing the prediction and generalization ability of models.

ii. Feature extraction: After pre-processing, ML extracts appropriate features from the TENG output signal data sets to construct effective and non-redundant feature values for target prediction. The feature values can help to construct the subsequent learning and induction process, it can also improve the expressiveness and generalization ability of the model. Feature extraction is a step to reduce dimensionality while maintaining integrity and accuracy of original datasets describing the TENG. Common feature extraction methods include feature selection, feature transformation, and feature construction.

iii. Model selection and optimization: According to the characteristics of TENG output signal and its application scenario, a suitable ML model is selected, the model is subsequently trained by the training data, and the model parameters are changed to make it better fit the data. After model training, the cross-validation method can be used to appraise the model performance and generalization ability, including accuracy, recall, F1-score, etc. Optimization should be carried out if the model performance does not meet the requirements, such as adjusting model parameters, increasing training data, changing feature engineering methods, etc.

iv. Model deployment and application: After model evaluation and tuning, the model can be deployed into actual application scenarios of TENG. As TENG generates new data, the trained model will be invoked to identify new data and achieve real-time prediction functions.

To sum up, the workflow of ML processing TENG output signal data includes data acquisition, data preprocessing, feature extraction, model selection and optimization, model deployment, and application. This process is an iterative process that requires continuous training, validation, and optimization to improve the performance and application effect of ML models.

4. Applications of TENG with Different ML Algorithms

4.1. Bayes, DT, and RF Algorithms

In the previous TENG signal processing process, researchers only set a threshold voltage for simple state judgment, when the peak signal output value is higher than the threshold value, the sensor is judged to be active. However, it is still difficult to set the appropriate threshold voltage. Improper threshold voltage will cause the signal crosstalk of adjacent units and reduce the detection accuracy of the sensor array. To address this problem, Jeon et al. used Bayesian decision rules to establish and verify decision boundaries for the maximum active unit (MAC) of TENG sensor

Table 1. The summary of the advantages and disadvantages of ML algorithms.

Algorithm	Advantages	Disadvantages	Applications
Naive Bayes	– Performs well on small datasets – Simple and efficient	– Feature independence may not hold in reality – Requires prior knowledge of probabilities	– Spam filtering – Text classification
Logistic Regression	– Simple and easy to understand – Fast training speed	– Limited ability to model complex relationships – Susceptible to noise	– Binary classification – Disease prediction
Decision Tree	– Handles both numerical and categorical data – No need for feature scaling	– Prone to overfitting – Sensitive to noise/outliers	– Pattern recognition
Random Forest	– Improves stability and accuracy of Decision Tree – Be able to handle large numbers of data features	– Longer training and prediction times compared to Decision Tree	– Medical diagnosis
K-nearest Neighbor	– Simple and intuitive – Suitable for small data – Applicable to multiclass classification	– Sensitive to outliers – High complexity	– Handwritten digit recognition
Support Vector Machine	– Performs well in high dimensional spaces – Effectively handles nonlinear relationships	– Inefficient for large datasets with many features	– Image classification – Text classification
Convolutional Neural Network	– Powerful feature learning for images and spatial data – Parameter sharing reduces the number of training parameters	– Less flexible in handling sequential data – Sensitive to input size and position	– Image recognition – Object detection
Recurrent Neural Network	– Handles sequential data well – Memory capabilities for capturing sequence context	– Difficulty in handling long-term dependencies, prone to gradient explosion – Slow training speed	– Language modeling – Machine translation

array.[97] The result shows that the accuracy of classification of daily activities and falls is as high as 95.75% when the intersection of the probability function (2.600) is selected as the decision boundary.

The Bayes model is simple and fast in predicting samples, with stable classification efficiency. It works well on slight amounts of data, which can also handle multiple classification tasks. However, the Bayes model is not effective in classification when the number of TENG signal channels is too large. Besides, it is also sensitive to the expression form of TENG output signal.

Compared with Bayes model, DT has more advantages in high dimensional data processing. The steps of learning and classification by DT are simple and efficient and it is not sensitive to the loss of intermediate value. Zhang et al. fabricated lightweight TENG sensors by screen-printing method to realize respiration monitoring based on DT.[98] In the training phase, 5 classification feature sets are established for each breathing behavior. Based on DT algorithm, the feature set and corresponding label are used to realize the training classification model. Through the Gini index, the importance of 12 features is analyzed. Among them, variance, root-mean-square, kurtosis, and unbiased estimation are the most important classification indexes. The results show that the average accuracy of identifying breathing types reached 97.2% (**Figure** 4a). Han et al. implemented self-powered fault diagnosis for rolling bearings based on TENG.[99] DT is used to identify faults in different parts through the TENG current. They also chose Gini index as the generation algorithm (the maximum depth is 30 and the minimum nodes is 5). The results show that the accuracy of identification is more than 92%.

By integrating multiple DTs together, a stronger classifier RF can be built. The algorithm uses multiple DTs to make decisions and generate the final output results, which can effectively diminish the impact of the outliers in the TENG signal. More importantly, the DT is prone to over-fitting due to using all features and samples, while the RF randomly selects several samples with putbacks, reducing the possibility of overfitting. Luo et al. designed a speech and gesture signal converter and greatly improved its sensitivity (167 mV dB^{-1}) by spraying silk protein on copper electrodes.[100] MEL Frequency Cepstral Coefficient (MFCC) is calculated to extract the feature values of the speech to construct the database and RF is selected to establish the speech pattern model. It has been observed that the normal human voice frequency is 50–500 Hz, but different person's voice frequency corresponds to different amplitude. By tracking each person's frequency information, RF is able to distinguish signals excellently, with 97.0% accuracy (Figure 4b).

Cheng et al. collected voltage data generated by the foot pedal TENG through time-sliding window (sampling interval 0.02 s) and stored them sequentially.[101] After collecting the signals of TENG and driving simulator, the unsupervised Gaussian mixture model is selected to cluster the samples automatically. Multiple candidate features are then extracted from the voltage data and sequenced to train the RF model. The results show that the classification accuracy of TENG data is more than 90% using the RF algorithm (Figure 4c), indicating that the integrated learning algorithm has higher accuracy in identifying the driver's pedal action. Jiang et al. used RF classifier to classify different sitting postures.[102] The collected 8-channel TENG signals are transformed by Fast Fourier Transform (FFT), and RF is used to

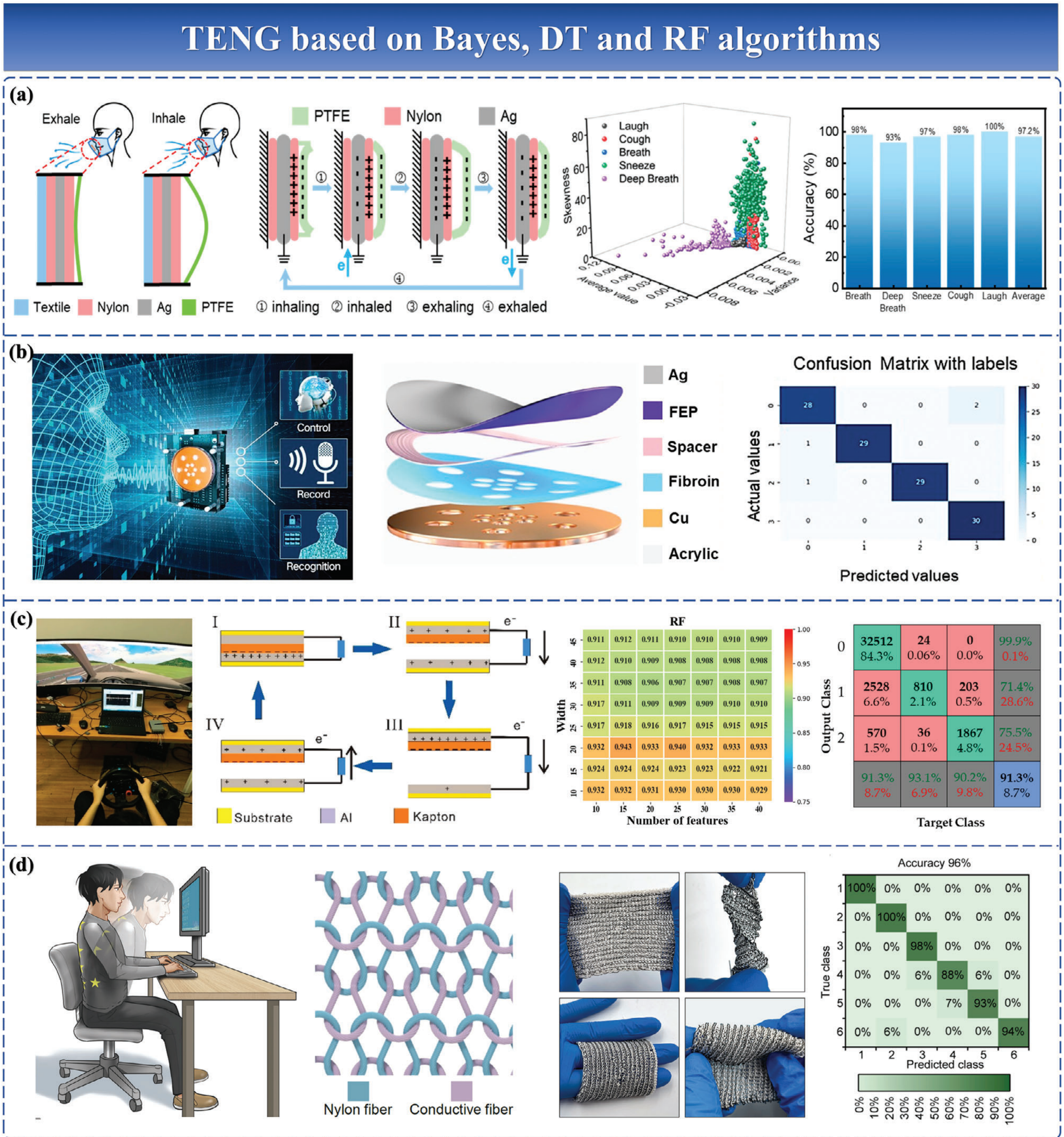

Figure 4. a) Structure and working principle of TENG sensor fabricated by screen printing, and the feature distribution and recognition accuracy of different breathing states by DT algorithm.[98] Copyright 2023, MDPI. b) The structure of TENG-based speech recognizer and the recognition accuracy of different human voice by RF algorithm.[100] Copyright 2023, American Chemical Society. c) The working principle of foot-pedal TENG and the recognition accuracy of RF for different driver identities.[101] Copyright 2020, MDPI. d) Structure of knitted TENG-sensing textiles and seated position recognition based on RF algorithm.[102] Copyright 2022, Springer.

randomly sample data rows and columns to form multiple training sets. Figure 4d shows that the accuracy of RF classification of the sitting position is as high as 96.6%, exceeding DT (94.3%) and Logistic Regression (95.5%).

4.2. KNN and K-Means Algorithms

K-Nearest Neighbor (KNN) is one of the simplest ML algorithms. It is an instance-based supervised learning algorithm, which does not need to be trained. Consequently, it is only necessary to select the appropriate parameter K, instead of a model that generalizes data features. Every time KNN is used for prediction, all the training data is involved in the calculation. The K value can directly affect the prediction effect and the optimal K value can be obtained by cross-validation method. KNN has the advantages of simple principle and wide application range. However, it also has the disadvantages of too much computation and slow prediction speed. Therefore, it is necessary to optimize KNN when using it.

Yang et al. designed pressure-sensitive insoles and smart ski poles based on 3D-printed Thermoplastic Polyurethane (TPU) as the triboelectric layer.[103] The sensor sensitivity is 0.054 V kPa^{-1}, demonstrating the TENG output have linear relationships with the external force. Subspace KNN is selected as the pattern recognition algorithm, the data set samples are randomly divided into multiple subspaces in accordance with the dimension. The subspace dimension is 6, and the results show that the four behaviors could be effectively distinguished with an accuracy of 98.2%. In addition, KNN is used to recognize three typical ski techniques. P-Find method is used to select the appropriate time interval as the input of feature extraction, and then KNN subspace is used to automatically classify sub-techniques. The results show that the technique can be completely recognized with almost 100% accuracy.

The cost of manual labeling will increase when the amount of sample data provided by TENG is huge. In this case, unsupervised learning method can be chosen to solve the problem. Common unsupervised learning methods include PCA and K-Means, which have the advantages of simple principle and fast convergence speed for clustering problems. Yun et al. fabricated a TENG mask combined with ML for facile sleep monitoring.[104] The TENG is made with the modified Acrylonitrile Butadiene Styrene as the mask frame and Polytetrafluoroethylene (PTFE) as the triboelectric material. Its voltage is 8.54 V, 7.89 V, and 7.12 V under shallow, normal, and deep breathing states. Depending on the FFT method and peak analysis algorithm, the respiration rate and signals are extracted and divided into the x and y axes respectively. The new data, by comparing the actual distance between the input and the centroid of different clusters, will be assigned to clusters closer to the centroid. The results show the classification accuracy based on K-means clustering algorithm is 87.17%. Moreover, classification by relative output voltage allows for more accurate identification of each sleep stage. When the weight value is multiplied by the respiration rate, and changed from 1.0 to 0.1, the classification accuracy will increase to 86.7%, 88.3%, 91.7%, and 96.7%, respectively.

4.3. SVM Algorithms

SVM is a linear binary classification algorithm belonging to supervised learning. The classification decision of SVM is determined by the support vector, which can capture the key data with high robustness. When the sample data output by TENG is small, SVM is more suitable to be selected to distinguish the data features. Kim et al. fabricated a catechol-chitosan-diatom hydrogel with high stretchability and ionic conductivity for self-powered tremor sensors to monitor Parkinson's disease patients.[105] When tremors occur, TENG generates voltage signals with a frequency of 1.7–10.3 Hz or even higher, and the signal power increases with the severity of the tremor. Therefore, the frequency and power characteristics of TENG can be used for detecting Parkinson's patients' health status. They use KNN and linear SVM to classify the test samples, and the result shows that linear SVM classify the data more accurately than KNN, with an accuracy of 100%.

Linear SVM is only available when the samples are linearly separable states in vector space. However, classification problems faced by TENG may be nonlinear in some cases, where linear SVM cannot accurately achieve classification function. By mapping the linear indivisible samples to the vector space of higher dimensions, nonlinear SVM can be obtained to realize the classification function. Liu et al. made a wearable keyboard based on silk fibroin protein electrodes and PTFE to collect current signals generated by tapping.[106] The currents generated by different people are different, and SVM is used to classify the currents and identify users. They chose the Radial Basis function (RBF) kernel as the SVM kernel to map the sample to the high-dimensional space, which is suitable for sample processing under nonlinear relations, making the data linearly separable. Appropriate penalty parameter C should be selected to avoid overfitting problems and misclassification when using RBF kernel. The value of C is adjusted to 1.0–2.0, and the highest classification accuracy is close to 90%. Zhang et al. designed a TENG sensor for detecting and identifying the liquids' leakage.[107] When liquid leakage is detected, TENG outputs current and constructs sample data. They also select SVM with RBF as the kernel function to classify water and NaOH. K-CV is used to optimize the kernel parameters C and G. One hundred twenty sample data are collected within 20 s and normalized within [0,1]. The result shows that the recognition accuracy of tap water and NaOH liquid is 95%.

The TENG signal may have the characteristics of multiple classifications, while the SVM algorithm is primitively devised for binary classification. Therefore, it is necessary to combine binary classifiers to construct multiple-classifier when dealing with multiple classification problems. Zhao et al. proposed an untethered triboelectric patch based on PTFE as triboelectric layer.[108] The sensor is attached to the index finger and then used to touch the object, as shown in **Figure 5a**. The response signal is transmitted through the human body to form a sensing data set, and the multi-classification SVM is used to assist in object recognition. The samples are divided into training and test groups, and the linear kernel is used during the SVM training process, showing a high accuracy of 94.9%, which proves that the sensor can effectively identify the objects for users.

Yang et al. fabricated a high bending angle resolution TENG extracting multi-dimensional signal features.[109] Three TENGs convert the finger flex into digital signals. Multi-classification SVM is generated by building multiple binary-classification SVM that distinguish three-channel signal patterns for one class of acquisition from the rest. In the process of real-time recognition, multi-classification SVM is selected to recognize users according to the input data characteristic patterns. It can be seen that the overall verification accuracy is 93.1% through the confusion matrix obtained by ten-fold cross-validation. Sun et al. classified human gait based on SVM and TENG by writing patterned MXenes ink electrodes directly onto the triboelectric material.[110] They extract physical and statistical characteristics such as

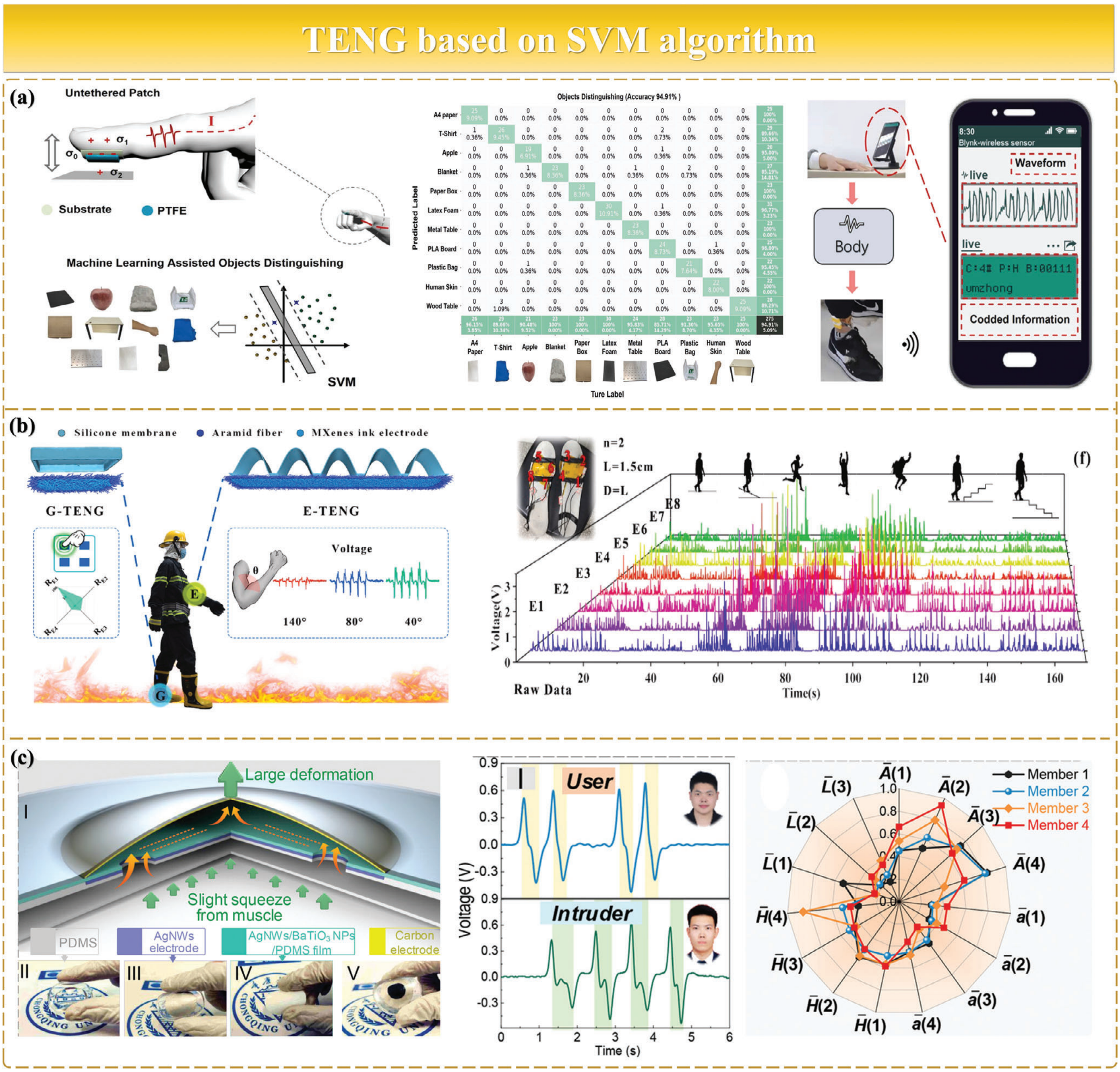

Figure 5. TENG applying SVM algorithms: a) The structure and principle of TENG as a patch sensor, and the accuracy of identifying objects using linear kernel SVM.[108] Copyright 2022, Elsevier. b) The structure of the pattern MXenes electrode TENG, and multi-classification SVM for 7 gaits identification.[110] Copyright 2021, Elsevier. c) The schematic of BTUSE, and the electrical signal and radar chart of user identifications.[112] Copyright 2021, Wiley-VCH.

amplitude, mean, standard deviation, and number of TENG. In the training process, the multi-classification SVM classifier adopts one-to-many strategy to classify gaits. Seven gaits (walking on flat roads, walking down slopes, running, etc.) can be classified with a good accuracy of 92.18% (Figure 5b). Tong et al. studied a wearable 3D-printed triboelectric device that generates different TENG output signals through membrane deformation caused by the user's face movement.[111] They train various ML models to classify words spoken silently. Among them, the linear discriminant analysis model has the lowest accuracy in word classification (74.8%). The classification accuracy of the SVM (98.4%) and KNN (98.1%) models is relatively high, while the Gaussian SVM model has the highest recognition accuracy of 99.2%.

The accuracy of SVM will decline when the sample data is large. Besides, SVM space consumption is chiefly used for storage of training samples and kernel matrixes. As the TENG output data is too large, the training data set will be particularly large, resulting in a long SVM training time. In this case, the dimension reduction method, such as PCA and t-Stochastic Neighbor Embedding (t-SNE), can be selected to perform feature selection and filter out the feature subset that has a great impact on the classification problem. It can effectively reduce the feature dimension and sample data size. Zhou et al. report a bionic TENG-based ultra-sensitive self-powered electromechanical (BTUSE) sensor for real-time human-computer interaction (HMI).[112] The system extracts the signal features through denoising and peak detection techniques, then uses PCA to extract the main features and remove the redundant information. Then, two classes of SVM classifiers are applied to construct the user profile database of main features. Figure 5c shows that the BTUSE sensor performs well in protecting user privacy and hands-free typing communication systems (96.3%). Ji et al. constructed TENG-based writing plates to obtain the original signal of the letters.[113] Due to the high dimensionality of the data, they used t-SNE to reduce the size of the data from 20 to 7 dimensions. The feature vector extracted is only relevant to the time series of signal patterns, thus avoiding the influence of different forces and frequencies on letter recognition. The results show that the Medium Gaussian SVM has the highest recognition accuracy (93.5%).

4.4. Deep Learning Algorithms

Deep learning is a branch of ML using deep neural networks to build more complex models, which have a deeper understanding of data. In the case of providing enough data, deep learning algorithms, compared with traditional ML algorithms, directly transfer data to the network without feature engineering, which greatly reduces the complexity of the process with strong adaptability.

In addition, deep learning is based on neural network structure, owning strong nonlinear fitting ability, which can map any complex nonlinear relationship. It has strong robustness, powerful self-learning, and memory ability. In general, deep learning neural network models are divided into supervised learning and unsupervised learning. The common models in supervised learning are Artificial Neural Network (ANN), Convolutional Neural Network (CNN), and Recurrent Neural Network (RNN), while in unsupervised learning are Generative Adversarial Network (GAN) and Deep Belief Network (DBN).

ANN, CNN, and RNN are common supervised learning neural networks. Among them, ANN contains input layer, hidden layer, and output layer, and only carries out forward processing on input, which is also known as feedforward neural network. Each layer of ANN tries to learn some weights, which has high classification accuracy, strong robustness to noise, and strong parallel processing ability. Zhou et al. developed a vector triboelectric sensor for detecting the vibration and rotation states of devices.[114] Based on the signal magnitude and phase characteristics generated by hybrid triboelectric sensor, they used a double-layer neural network to identify the vibration frequency (96.5%) and direction (95.5%) of the device, surpassing Logistic Regression and Linear Regression, as shown in **Figure 6**a.

Xiao et al. fabricated a hybrid electronic skin containing a flexible pressure sensor and TENG that perform highly sensitive exploration of both static and dynamic pressures.[115] They induct a high-speed Field Programmable Gate Array (FPGA) data collector and a multi-layer perceptron (MLP) model to form a material perception system, achieving real-time perception of materials with unclear forms and smooth surfaces. The generated signals are collected and fed into the trained MLP model, which can separately identify the type of material and its position on the board. The system can identify 12 kinds of materials' indistinguishable surface with an accuracy of 98.9% (Figure 6b). Zhang et al. constructed a TENG sensor with TPU-coated polyester, Si rubber, and conductive Ni fabric, and combined it with an ANN prediction model to achieve gait analysis.[116] The hardware circuit composed of Analog-to-Digital Converter and Microcontroller Unit is used to collect and process the sensor output voltage, FFT is used to eradicate the information of the time domain. Afterward, the samples are directly imported into the ANN for training. To enhance robustness, they insert the Dropout and Batch Normalization layers into the first Fully Connected Layer (FCL), with the last FCL outputting the predictions. The results show that the accuracy of gait recognition is 98.4%. Yao et al. fabricated a sound-driven TENG sensor composed of Fluorinated Ethylene Propylene (FEP) and conductive fabric.[117] They use MFCC to extract the one-dimensional voltage signal characteristics of the TENG. Here, DNN is used to identify different people's voices. Each hidden layer has 512 neurons, an activation function Rectified Linear Unit (ReLU) for avoiding gradient disappearance problems, and a Dropout function for preventing overfitting. In addition, Adam optimizer is selected to sparse gradients. Figure 6c shows that after the model training, the recognition accuracy of new voice data reaches up to 99%.

In addition to using DNN in different applications, researchers also use it to predict and optimize the performance of TENG itself. Jiang et al. used DNN innovatively to predict TENG performance under diverse structures and conditions.[118] The width of the grating, the outer radius of the disk, and the rotation rate generate suitable data sets for DNN, consisting of an input layer, three hidden layers, and an output layer (Figure 6d). After using SGD algorithm, the final loss value of DNN model can be reduced to 0.0435. The predicted output power of TENG is in alignment with the experimental value, which will be of great help in designing experiments.

ANN is easy to implement and understand, and can effectively handle nonlinear data. However, ANN typically employs a fully connected structure, where each neuron is linked to each neuron in previous layers, resulting in a large number of parameters and computations, making training and reasoning more time consuming. Besides, there are too many parameters of ANN as the amount of signal data output by TENG is small, which is prone to overfitting problems.

CNN use convolutional layers to capture local features of input data, and parameter sharing allows the network to learn common features, reducing model complexity and training time. Meanwhile, it achieves spatial invariance through the pooling layer, and the network can still correctly identify the input even if there is deformation.

Therefore, compared with ANN, CNN has fewer parameters, faster calculation speed, and better performance on data with spatial structure and large-scale data sets. Li et al. combined the triboelectric sensing unit with the electromagnetic sensor to create the hybrid tactile sensor for object detection.[119] They use a one-dimensional CNN (1D-CNN) for dual-mode signal handling and data analysis. The sensor-equipped robot picked 8 fruits 200 times, generating signals that are fed into the 1D-CNN for identification. The results show that as the training

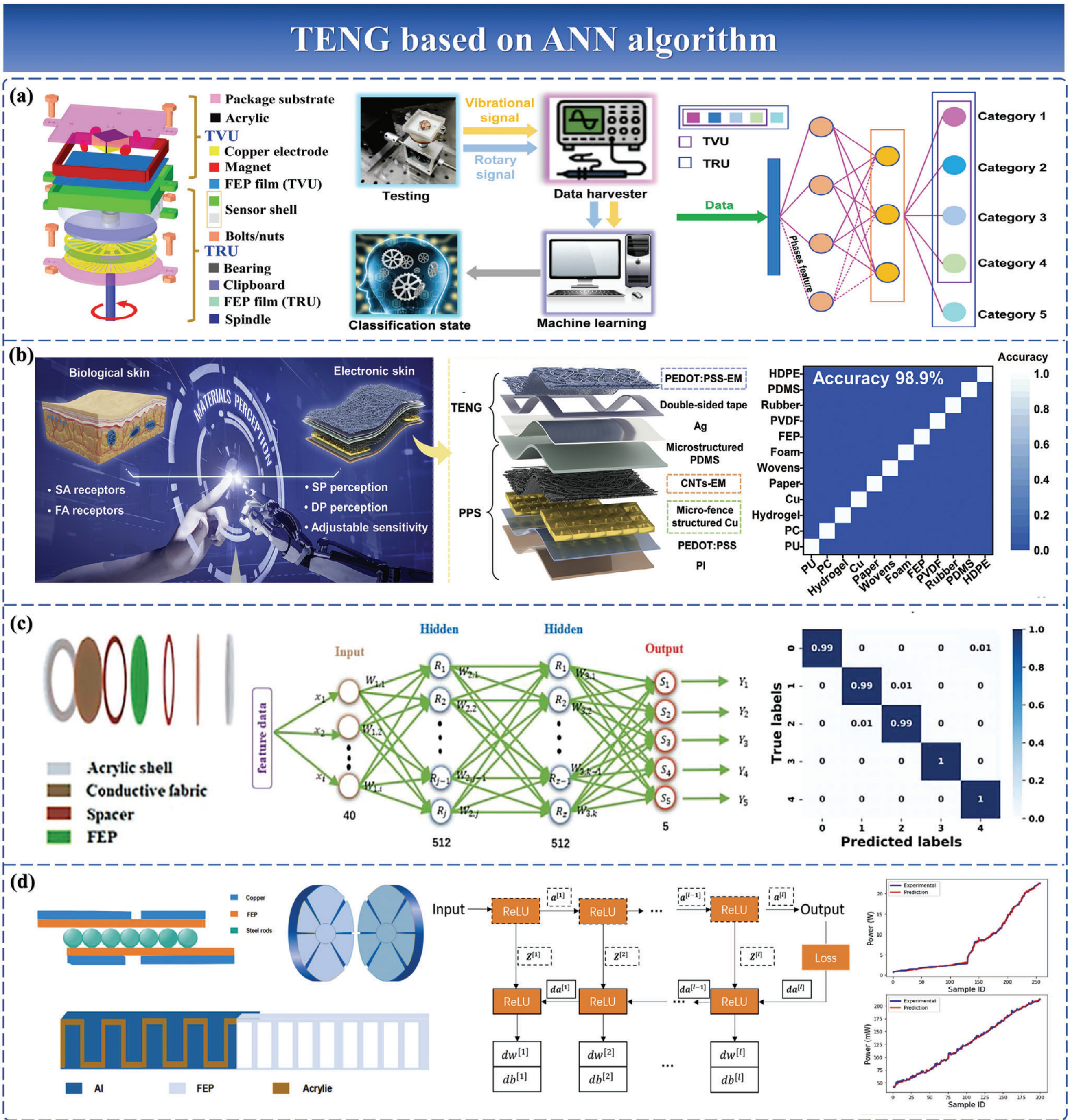

Figure 6. TENG applying ANN algorithms: a) The structure of TENG, and the recognition process based on ANN.[114] Copyright 2023, Springer. b) Schematic and structure of electronic skin, and the recognition accuracy of different materials based on ANN.[115] Copyright 2022, Elsevier. c) The structure of sound-driven TENG sensor, schematic of ANN, and the recognition accuracy for different people.[117] Copyright 2022, Wiley-VCH. d) TENG of different structures, ANN structure, and comparison between predicted and measured curves.[118] Copyright 2022, Elsevier.

iterations reach 20 times, the accuracy tends to converge (94.6875%–99.6875%), and the identification accuracy of different fruits reaches up to 98.8% (**Figure 7a**). Feng et al. sprayed Carbon Nanotubes (CNTs) onto polyester textiles and obtained superhydrophobic textiles through ethanol etching process, forming TENG with ECOFLEX for gesture recognition.[120] TENG sensor is linked to Arduino for data acquisition, and Python is used to process the acquired data in real time to achieve functions such as shooting game control through gesture recognition. 1D-CNN has an input size of 10*200 and an output size of 4. Each gesture takes up 10 channels to analyze the signals from all fingers, and the recognition accuracy is 99% (Figure 7b). Zhu et al. constructed a

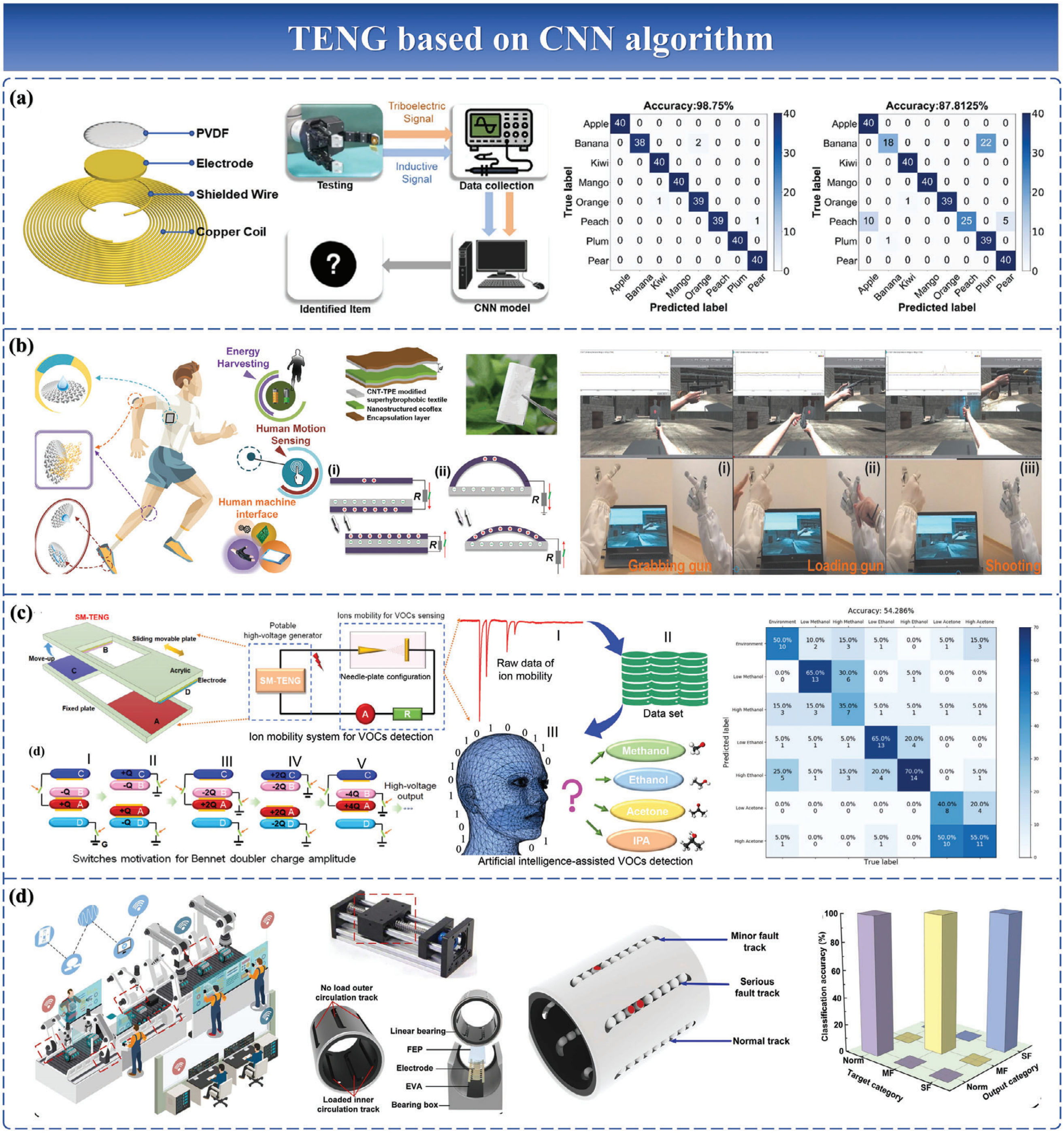

Figure 7. TENG applying CNN algorithms: a) The structure of triboelectric-electromagnetic sensor, the process, and accuracy of fruit recognition based on 1D-CNN.[119] Copyright 2022, Elsevier. (b) Schematic diagram, structure, and working principle of super hydrophobic TENG, 1D-CNN's gesture recognition implementation for shooter game control.[120] Copyright 2020, Wiley-VCH. c) Ion mobility analyzer powered by TENG, and the identification of volatile organic compounds by 1D-CNN.[121] Copyright 2021, Elsevier. d) The schematic diagram and structure of triboelectric linear bearing sensor, and the classification accuracy of bearing faults.[124] Copyright 2023, Elsevier.

TENG-powered ion mobility analyzer.[121] The four-layer 1D-CNN is used to identify various volatile organic compounds, such as acetone, methanol, and ethanol, with the highest identification accuracy (ethanol) of 70% (Figure 7c).

1D-CNN is commonly utilized for processing sequential data, such as text, time series, and sound data, while it requires data to have a certain continuity in the timeline. Therefore, in some TENG applications, data preprocessing and feature engineering will become cumbersome and complicated, leading to a decline in the recognition effect of 1D-CNN.

2D CNN (2D-CNN) model is mainly used for image classification. Compared with 1D CNN, it uses convolution and pooling to capture spatial features in images, which enables it to learn more complex feature representations and have better migration effect. Wei et al. fabricated a triboelectric tactile sensor array.[122] They convert the signal waveforms generated by the TENG array into picture format, and use VGG image recognition technology to identify nine different materials. VGG is one of the symbolic networks of CNN. It is further revised on the basis of AlexNet model, and more abstract features can be extracted when dealing with graphs. The results show that the total accuracy of material identification reaches 96.62%. Beigh et al. used photo-patternable Barium titanate (BTO) to construct a piezoelectric-triboelectric sensor array on a flexible substrate.[123] The mixed output mapping of the 6*6 sensor matrix is input into the Adam-optimized 2D-CNN model, and the posterior foot deformity detection is realized with an accuracy of 98.84%. Qin et al. fabricated a triboelectric linear bearing sensor (TLBS) based on FEP and interdigital Cu electrodes for bearing operating condition monitoring.[124] They also use Continuous Wavelet Transform (CWT) to convert linear bearing signals into time-frequency graphs, and 116 CWT graphs are obtained for each signal type. The bands on the CWT maps of normal signals are complete, while the bands of fault signals are defective. The time-frequency graphs are directly imported into CNN as feature images, and Batch Normalization and Dropout are selected for reducing model overfitting. After 100 iterations, the t-SNE visualization proves that the model can effectively distinguish different data types with 100% accuracy, as shown in Figure 7d.

CNN shares convolution kernel in the training process and automatically extracts features, that can efficiently process high-dimensional data. However, as the network depth is too deep, Back Propagation will lead to the parameters of the input layer spread too slow. A great deal of valuable information will be lost, and the correlation between the local and the whole TENG signal will be ignored.

Relatively, the output of RNN is correlated with the previous output, and the network memorizes the previous information and applies it to the current calculation. The signal generated by TENG is a waveform that changes over time, and every second of data is correlated. For instance, in accordance with the positive and negative gradient of the waveform near the peak, it can be determined whether the current signal point is in the front position or the rear position of the peak signal, which helps to further enhance the prediction ability of the model for the peak distribution.

By circulating neurons, RNN can process sequences of different lengths at different times. Besides, the introduction of Long-Short Term Memory (LSTM) and Gate Recurrent Unit (GRU) structure can effectively resolve the gradient disappearance or gradient explosion problems, capture long-distance dependence, and improve the recognition accuracy. They are widely used in semantic recognition, natural language processing, and other fields. Lu et al. built highly sensitive sensor based on Polyvinyl Chloride (PVC) and Nylon films to generate signal outputs under different amplitudes and frequencies by muscle movement.[125] Expansionary RNN are used to identify different lip movements. The training sample in the deeper feature space is obtained by the feature extractor, which is a multi-layer extended RNN for capturing long-term dependencies in a sequence. The expansion principle effectively reduces model parameters and significantly improves the training efficiency. In particular, GRU is selected as the basic units of RNN, including update gates and reset gates for capturing dependencies in the sequence. Based on Expansionary RNN, they collect and compare the lip movements of vowels, words, phrases, and silent speech, and **Figure** 8a shows that the identification accuracy reaches up to 94.5% after 20 epochs. Ye et al. developed a sheath core TENG yarn based on electro-assisted core spinning technology, which consists of rough dielectric surface and conductive core yarn.[126] The RNN, based on classification coding, predicts the type of contact material through the peak distribution of output voltage.

The integration of CNN with RNN, known as Convolutional-Recurrent Neural Network (CRNN), has great advantages when processing sequence data and image data. Among them, RNN is used to process sequence data and time sequence information, and CNN is used to process image data and capture spatial features. The union of them can effectively take into account the time dependence and spatial structure of tasks. It fits very well with the output signal generated by TENG, which can dissect the amplitude and frequency information of the output signal over time, and effectively capture the spatial characteristics of the waveform input in the image format.

Therefore, CRNN has higher precision and accuracy in the processing of TENG output signals. It can effectively reduce the overfitting and improve the model generalization performance.

It should be noted that the design and adjustment of the CRNN framework is critical. The structure and hyperparameters of CNN and RNN need to be carefully balanced in conformity with the task nature and the data characteristics, so as to adapt to the processing tasks of TENG output signals in different structures and applications. Mao et al. used ECOFLEX/polyvinyl alcohol (PVA)/graphitic carbon nitride (g-C_3N_4) to fabricate TENG.[127] They built a CRNN model based on the integration of CNN with GRU to secern the small differences between the detected output voltage peaks for identifying four different balls in real time. The CNN layer excerpts local features, and the GRU captures long-term dependencies in the data. The reset gate and update gate help the GRU determine when to send past information to the future state. Therefore, the model can utilize CNN and GRU to identify the signal differences among the 4 balls. After 30 epochs of training, the model accuracy converges to 1. The prediction result shows that the CNN-GRU model can identify similar, different balls efficaciously, with an average prediction accuracy of 96.8% (Figure 8b). Xu et al. proposed a double-sandwich structure TENG sensor, which can detect small physiological signals and be applied to plantar pressure sensing.[128] They implement a human motion recognition system based on the CNN-GRU model, which can identify and classify four different motion actions with an accuracy of up to 99.42%.

Furthermore, Unsupervised deep learning techniques, particularly GAN and DBN, have demonstrated significant potential in expanding datasets for TENG. GAN can produce high-quality data through the adversarial process between generators and discriminators. DBN can extract rich hierarchical features from unlabeled data, with robust generalization

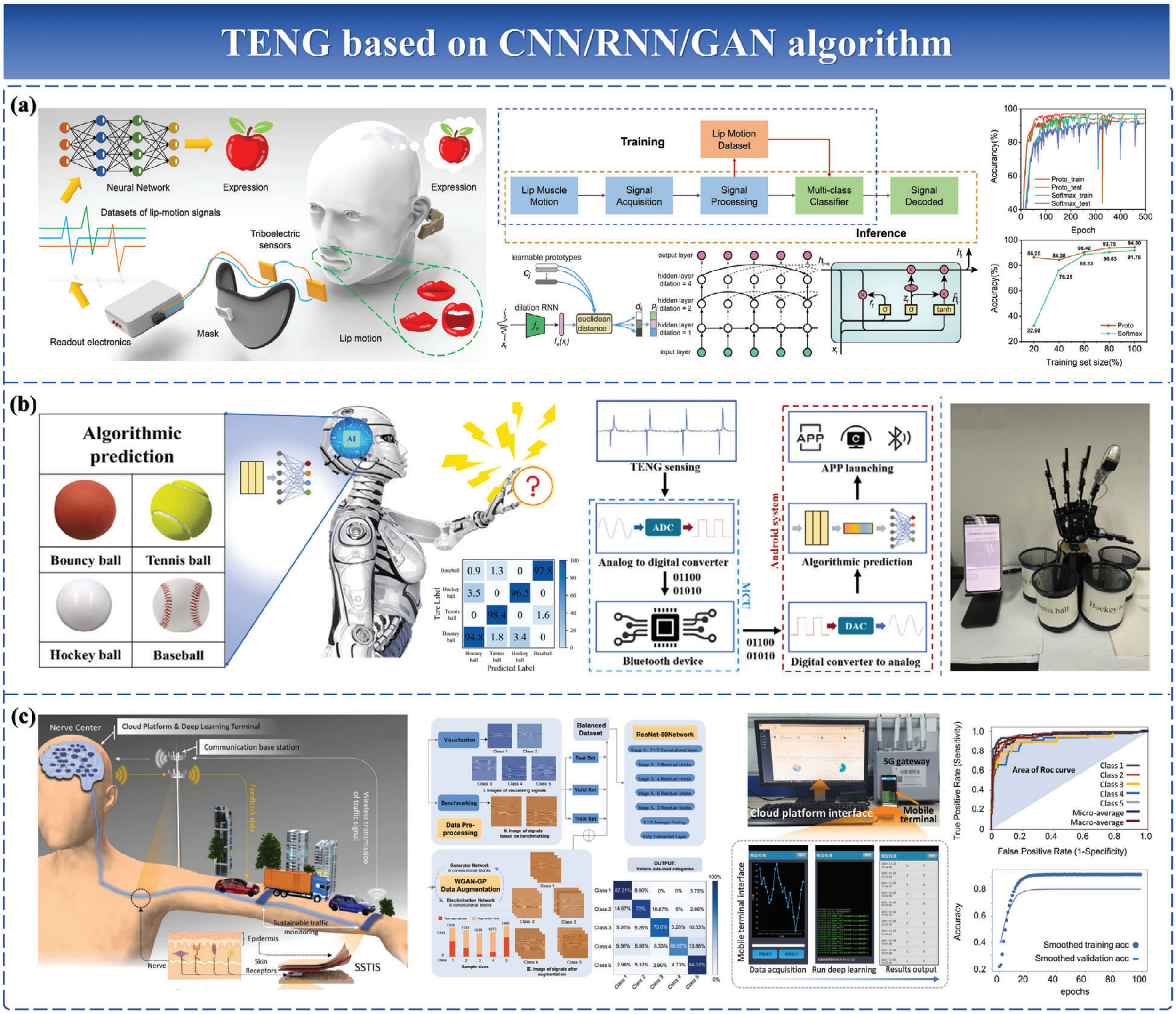

Figure 8. TENG applying CNN/RNN/GAN algorithms: a) Concept diagram of PVC-Nylon-based film sensor for lip recognition, and the working process and accuracy of RNN.[125] Copyright 2022, Springer Nature. b) The schematic diagram of TENG for sphere recognition, and the process of CNN-GRU.[127] Copyright 2023, Elsevier. (c) Bionic intelligent transportation system with PTFE-rubber flexible TENG sensor, and the network structure and recognition accuracy of CNN, RNN, and GAN ensemble.[129] Copyright 2022, Elsevier.

capabilities. However, due to the high complexity of training and slow convergence rates, there is currently a lack of research integrating DBN methodologies with TENG technologies. Compared to DBN, there has been more research on integrating GAN with TENG technologies. Zheng et al. further combined CNN, RNN, and GAN and applied them to TENG-based smart transportation bionic systems.[129] The flexible TENG sensor based on PTFE-rubber is installed on the road. The TENG sensor generates signal transmitted wirelessly to the neural network when vehicles pass by. They first collected data under four different vehicle loads and used LSTM in RNN to excerpt and handle the signal features of ≈2 140 160 pieces of signal data (the accuracy is 89.06%). However, the number of samples for multi-axle vehicles, compared with common two-axle vehicles, is very small in the research. The inspection accuracy is only 80.14% using the ResNet-50 model in CNN alone. In order to puzzle out the problem, they build a GAN-CNN deep model, and first used the generator and discriminator of GAN to perform data enhancement operations to generate a more balanced data set. Afterward, ResNet-50 is used to sort the data. The WGAN-GP-enhanced balanced data set is input into the ResNet-50 model. The results show that the combined network of WGAN-GP and ResNet-50 has better discrimination ability for two-axle vehicles or multi-axle vehicles, reaching 87.31% and 84.02%, respectively (Figure 8c).

5. Applications of TENG in Different Scenarios

5.1. Application of TENG in Health Care and Monitoring

Human beings never stop the pursuit of more excellent ways to improve health, but now sub-health is becoming increasingly prevalent in the society, and the aging population also poses great challenges to the medical and social welfare systems. Real-time monitoring of health and behavior, which can help prevent, diagnose, and treat a wide range of diseases, is receiving increasing attention. TENG has great potential for health and behavior monitoring owing to its high energy conversion productivity, light weight, high flexibility and good biocompatibility.

Ji et al. combined TENG and ML to develop a cardiac pharmacological evaluation platform. PDMS and Cu cores (3 μm gap) are used as triboelectric materials to form CPM-TENG for sensing the activity of cardiomyocytes.[130] When the cardiomyocyte is subjected to different drugs, its cyclic contraction and relaxation are different, so the electrical signals generated by CPM-TENG are different. Five features are extracted from signals, and after dimension reduction by t-SNE, SVM is used to identify and classify 10 drugs with an average accuracy of 98.5%, which proved the feasibility of TENG for pharmacological evaluation in vitro. Zhang et al. demonstrated an AI toilet consisting of 10 textile-based triboelectric sensors mounted on the toilet seat.[131] Based on the pressure distribution to obtain biometric information, the deep learning algorithm can correctly recognize 6 users (90%). Meanwhile, the system integrates the camera sensor to analyze the urine for monitoring the user's health status, as shown in **Figure 9a**.

In order to enhance the compliance and biocompatibility of TENG in human body and avoid skin trouble and allergy, Kim et al. fabricated a stretchable and self-healable catechol chitosan-diatom hydrogel for monitoring the health status of Parkinson patients.[105] SVM is used to judge the tremor degree (normal, mild, severe) according to magnitude and frequency of TENG signals, and the recognition accuracy can reach up to 100%.

An et al. integrated flexible Si rubber TENG onto a neck ring to generate voltage signals with different characteristics through different neck movements, representing different motion states.[132] They identified 11 types of neck movements based on CNN, including eight bending directions, one stationary state, and two twisting directions, with an identification accuracy of 92.63%, effectively realizing neck monitoring and rehabilitation assistance. Babu et al. built a nylon-based wearable sensor in combination with ML to classify/predict different hand postures, helping in the early assessment of neurological disorders, such as Parkinson's disease, multiple sclerosis, and other neurological disorders.[133] The classification and prediction accuracy are as high as 98%. Tong et al. fabricated a 3D-printed elastic metal core TENG fiber based on Si–Cu for monitoring organ edema and recognizing speech.[111] The 3D-printed mesh TENG fiber membrane on the kidney surface demonstrated its ability to detect edema during organ preservation in vitro. Besides, TENG fiber film is integrated into the surgical mask to identify mouth shapes through the electrical output generated by facial movements. The word classification accuracy of Gaussian SVM model is the highest, reaching 99.2%. Ye et al. provided a dual model temperature adjustment effect for the body and its environment (T-TENG).[134] The cooling material composed of Polyacrylonitrile/Barium Titanate (PAN/BT) and the heating material composed of Polyacrylonitrile/Carbon Black (PAN/CB) are fabricated, which actively realize the local monitoring and control of human body temperature. In addition, Morse code recognition in human motion is realized based on T-TENG, as shown in Figure 9b. Four algorithms are selected to investigate the identification accuracy of TENG signals. The recognition rates of DT, Extra Trees, RF, and SVM are 96%, 97%, 100%, and 100%, respectively. Zhu et al. also used 3D printing technology as the gait monitoring device to reflect the health condition during walking.[135] ANN and fast FFT are used to identify characteristic peaks in the output signal of TENG, where frequencies can be precisely transformed to recognize people. The peak search algorithm is utilized to detect the extreme point exceeding the threshold as the induction signal. Figure 9c shows that the trained ANN model is successfully used for gait recognition, weight monitoring, and robot sensing. Yun et al. fabricated an M-TENG applied to detect head posture and snoring.[104] Through unsupervised learning K-means clustering, sleep stages are classified according to the output signals (87.17%), which is of great use for monitoring sleep stages and helping to improve sleep disorders (Figure 9d). Li et al. used Kapton as the frame to support PTFE with Cu-attached backs to form a 6-layer parallel structure TENG, which was embedded into an intelligent carpet for gait identification.[136] Residual Dense-BiLSTM is used for multi-channel gait recognition, and the system can effectively detect a variety of human activities (98.0%) and distinguish the walking patterns of different individuals (97.0%).

5.2. Applications of TENG in Fault Detection

While paying attention to people's own health, the impacts of environment on human health are also important, and environmental problems are becoming increasingly important. In order to better solve the problems, the monitoring of the environment, such as water quality monitoring, air detection, and soil monitoring, is infinitely significant, which can help us accurately grasp the ecological environment changes and various indicators.

To address the problem of suspended sediment affecting water quality, Yang et al. fabricated droplet-driven TENG to realize sediment monitoring.[137] The main peak of TENG output is generated by contact between liquid and PTFE, and the irregular small peak is generated by contact between sand and electrode. They successfully identified particle size and mass scores based on CNN. For different particle sizes of sand, the recognition accuracy is more than 99%. The accuracy of particle concentration identification is relatively low, but still reaches 86.87%. Yu et al. further developed a dual objective recognition model to achieve recognition of particle type and concentration.[138] The TENG output signal is first used for particle type identification, and then the concentration recognition model is invoked to recognize the corresponding particle mass fraction. Finally, the accurate identification results of particle type and mass fraction are displayed. The identification accuracy of different particle types is more than 90% (**Figure 10a**). Zhang et al. fabricated P-type silicon triboelectric layer liquid-solid TENG.[107] On the basis of the different conductivity and wettability of the liquid, the short circuit current of TENG in response to liquids are different. SVM is used to identify liquids. The identification accuracy of tap water and NaOH liquids is 95.0%, and the classification accuracy of other liquids is more than 90.0% (Figure 10b).

In addition to the detection of liquid leaks, gas-based monitoring is also being studied. Zhu et al. fabricated triboelectric textile based on inkjet printing technology to power graphene

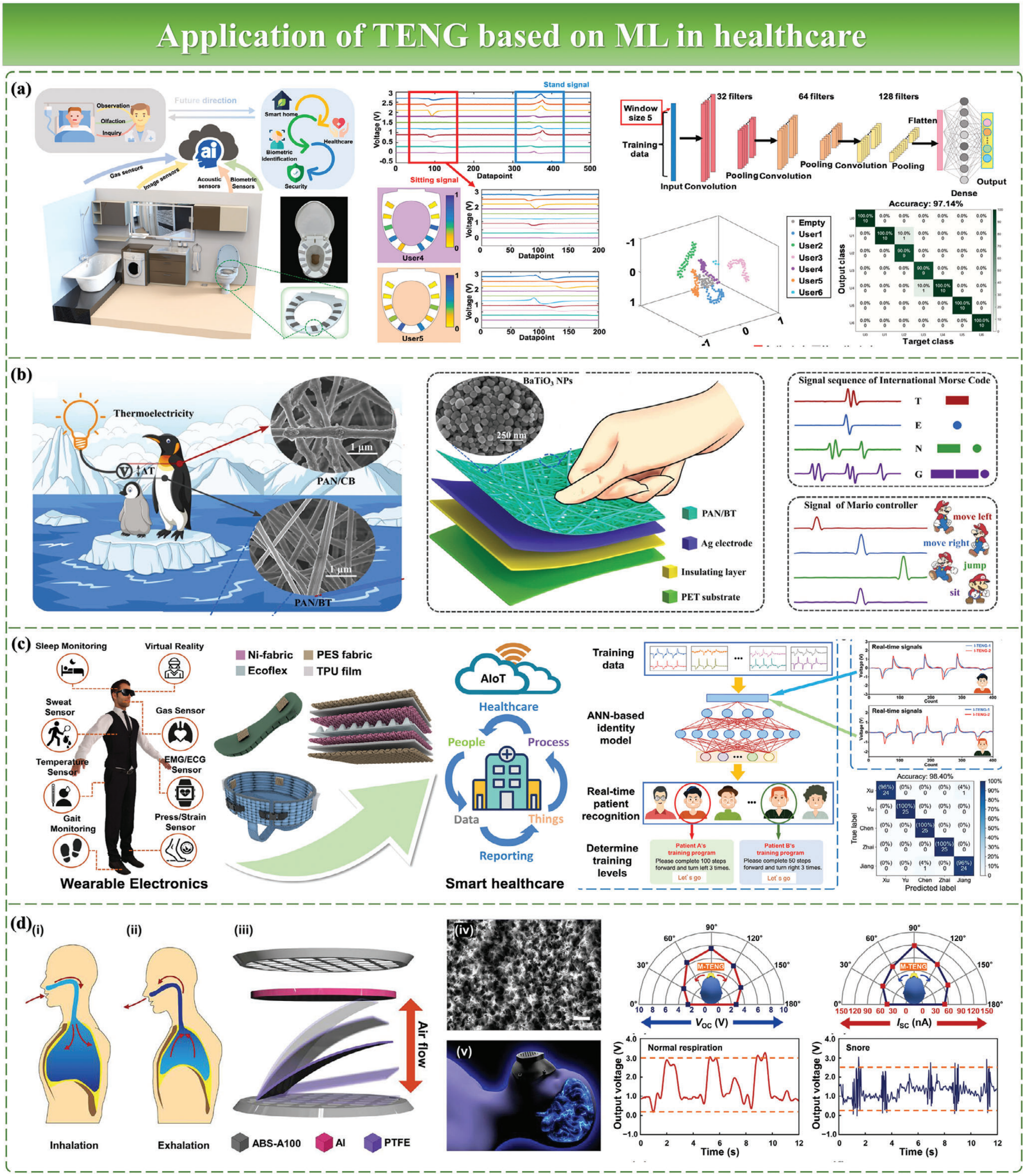

Figure 9. TENG-ML applications in healthcare: a) Schematic diagram and signal characteristics of intelligent toilet TENG, and user identification by CNN.[131] Copyright 2021, Elsevier. b) Concept diagram, structure, and signal characteristics of temperature management TENG.[134] Copyright 2022, Elsevier. c) Schematic diagram and structure of gait sensor, and ANN-FFT to achieve different user gait health.[135] Copyright 2022, MDPI. d) Structure of the breathing mask, and the signal output in different breathing states.[104] Copyright 2022, MDPI.

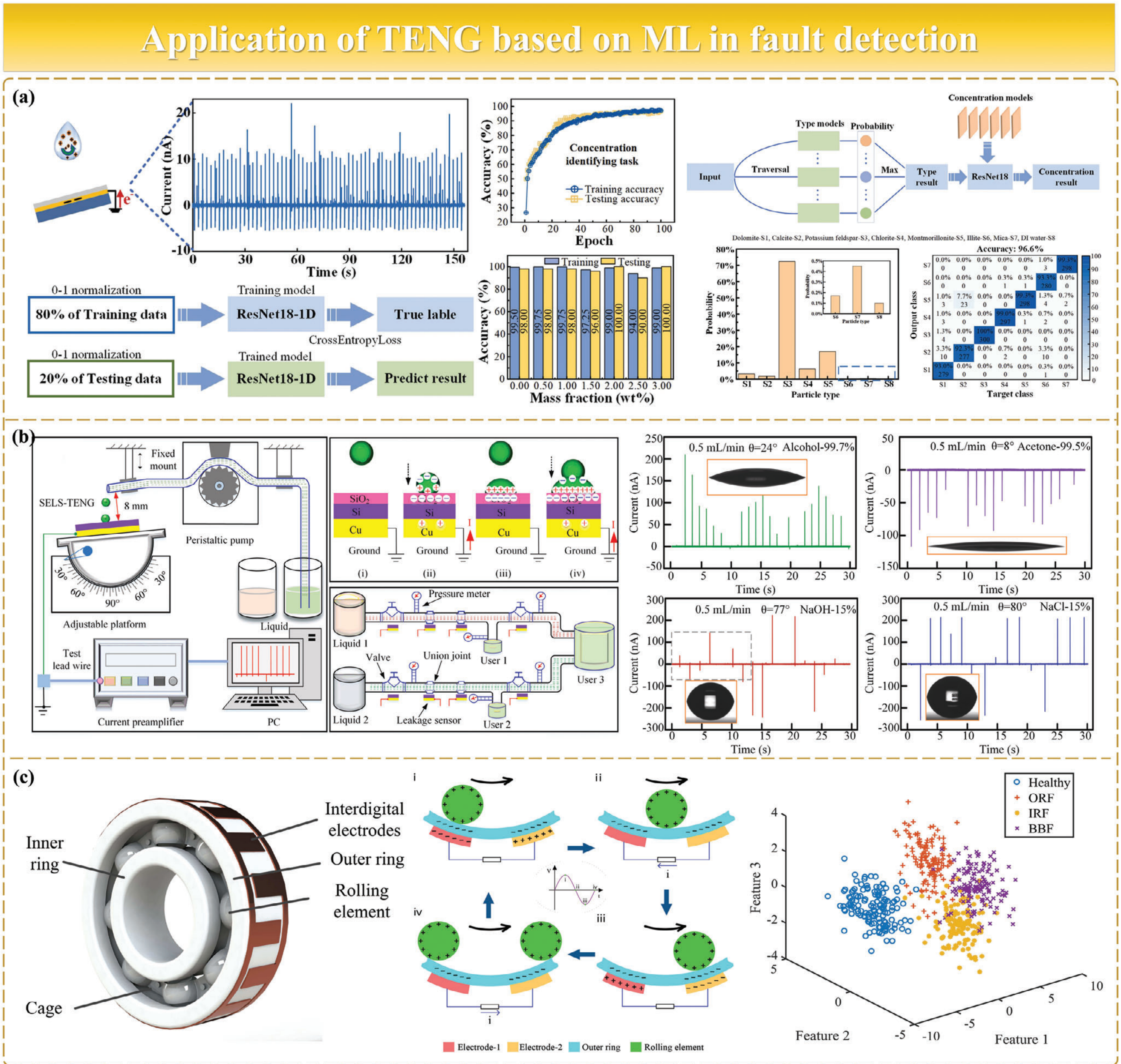

Figure 10. TENG-ML applications in fault detection: a) Principle and signal diagram of liquid monitoring sensor, and the detection accuracy of ResNet18 for different liquid leakage.[138] Copyright 2022, Elsevier. b) Schematic diagram, working principle, and signal output under different liquids of the liquid leak detection TENG.[107] Copyright 2019, Elsevier. c) The structure, working principle, and signal feature map of the bearing detection TENG sensor.[99] Copyright 2022, Elsevier.

gas sensors, combining with ML algorithms to monitor H_2 content in the air.[139] As the concentration of H_2 increases or decreases, the structure of the atoms in graphene/Pd changes during the adsorption/desorption of H, resulting in a change in current. PCA is used to visualize the raw data, and the concentration of each H_2 is decoupled into data points in two/three-dimensional space. Thus, the two-dimensional clustering method based on PCA uses cluster points to identify different H_2 concentrations effectively. Hasan et al. used the transient high voltage output (kV) of multilayer TENG to obtain plasma discharges of various gas molecules.[140] By configuring additional collector plates, the transient properties of different gas molecules are successfully collected, which are attributed to their differences in ionic mobility. They use a shallow neural network to classify 4 different gases with high classification accuracy under mixed conditions, which can be effectively used for gas leak detection. Zhu et al. used TENG to power the ion mobility analyzer and combined ML for the detection of various volatile compounds such as methanol, ethanol, and acetone.[121] Based on the unique characteristics of ion discharge patterns, such as peak number, frequency, and amplitude, different volatile compounds can be effectively identified.

In addition to monitoring the environment, the detection of intelligent devices is equally important. With the progress of technology, the structure of equipment is becoming more complex, and the automation degree is becoming higher. However, the equipment may have various failures and lose the intended function, causing economic losses, casualties and environmental pollution.

Therefore, fault detection is paid more and more attention. Han et al. glued flexible interdigital electrodes to the outer ring of a rolling bearing to form a rolling-type free-standing mode TENG for self-powered fault diagnosis of rolling bearing,[99] as shown in Figure 10c. When the fault occurs at different positions of the rolling bearing, the current spectrum of output signal is different. Therefore, SVM, DT, RF, Adaboost, and CNN are applied to classify bearing faults. The results show that the precision of five algorithms is above 92.0%. Among them, the accuracy of CNN algorithm can reach 99.38%. The team further proposed a pre-bent membrane-based TENG for fault diagnosis in rotating machinery.[141] After analyzing the characteristics of TENG output current, CNN model is constructed to sort bearing faults and mixed gear bearing faults. The accuracy of classification is also more than 92.0%.

Moreover, TENG itself is an excellent sensing device. In order to provide a stable working environment for TENG, most TENGs are designed with sealed structures that isolate them from the external environment, making it impossible to directly monitor their operating conditions. Shen et al. built a lightweight ANN, which shows low complexity and high sensitivity to signal waveforms, for interface defect detection and recognition of TENG.[142] The model successfully identifies 6 types of defects, with a high accuracy of 93.6%, which provides a new strategy for the fault detection and intelligent application of TENG.

5.3. Applications of TENG in Human–Computer Interaction

HMI is the bridge between humans and machines, playing a key role in achieving efficient coordination between humans and the digital virtual world. Traditional HMI, such as keyboard, joystick, and touch screen, can meet the needs of most scenarios,[143–145] while limited by power supply, complex structure, etc. TENG, as the self-powered sensor, has the advantages of low cost, simple structure, and wide selection of materials. It has been widely used for HMI functions, such as keyboards and touchpads.[146–148] However, it is far-fetched to characterize the signal diversity only through a single voltage output of TENG, and the complexity in the structure and electrode design will add additional power consumption and affect user convenience. Contrarily, crosstalk often exists in multi-channel sensing. Therefore, it is necessary to solve these problems for achieving accurate and real-time multimodal HMI.

The finger-motion-based HMI has high precision and multi-degree of freedom control that can recognize signals and map them to different commands. Yang et al. designed TENG based on PDMS and silicone rubber, and combined it with wireless customized Printed Circuit Board (PCB) to construct the glove system.[109] Three TENGs convert finger bends into digital signals, corresponding to three digits in accordance with the amplitude of the signal valley. Multi-classification SVM is used to construct the user portrait and identify them according to the characteristics of input data, with a verification accuracy of 93.1% (**Figure 11a**).

Ge et al. proposed a flexible microfluidic triboelectric sensor.[149] The bending of the finger squeezes the fluid chamber and the liquid enters the microfluidic channel. Each 10° bend of the finger adds a crest to the output waveform. They use CNN to identify the data of different wave peaks and then identify the corresponding gestures with 99.2% accuracy.

Zheng et al. presented a new flexible TENG sensor consisting of elastic bandage, silica gel, and carbon nanotubes.[150] The sensor has good stretchability (502%), which can be attached to the toe extensor muscle of the forearm to collect the gesture signals. LSTM is used for gesture recognition, and the accuracy of three-finger grip, four-finger grip, and one-index finger extension is 98.3%, 100%, and 96.7%, respectively (Figure 11b). Wen et al. assembled CNT/TPE into textiles to produce a super-hydrophobic textile TENG with higher moisture resistance.[151] CNN is used to recognize sign language words, maintaining high recognition accuracy even in high-humidity environments. Zhang et al. designed a microdome high sensitivity TENG based on $CaCl_2$/PVA/keratin and ECOFLEX, which can effectively recognize finger bending, gesture, and object shape based on SVM, transformer, and Res-Net.[69] Syu et al. used the near-field electrospinning process to fabricate the PCB-piezoelectric sensor and a Cu-triboelectric sensor, constructing bionic hybrid self-powered sensor.[152] LSTM is used in the context of gesture identification and effectively distinguishes five human actions satisfactorily (82.3%). Yang et al. fabricated a triboelectric-piezoelectric sensor made of PVDF electrospun nanofiber and mesh piezoelectric film for gesture recognition and switch control.[153] They use CNN to recognize gestures directly and Adam optimizer to avoid gradient redundancy. The accuracy of gesture recognition can reach 94.16%.

In addition to gesture recognition, a handwritten signature is also one of the important biometric personal behavior characteristics, occupying a special position in biometrics. It is widely used to verify personal identity and enhance security and privacy. Online signature can collect the speed, acceleration, inclination, and writing force of notes, but it is not easy to use and has high cost. Offline signatures are easy to access but have low accuracy. Therefore, there are still some problems to be solved in handwritten signature verification. The surface texture technique can effectively improve the output characteristics and sensor sensitivity,[154–156] while ML can effectively extract and analyze the features of handwritten signals, which makes TENG-ML show great potential, as an intelligent self-powered writing pad, in recording handwritten signals.

Inspired by bischofia polycarpa, Zhang et al. molded the same micro/nanostructure on PDMS to form a TENG writing pad with Cu electrodes.[157] The TENG-based handwriting pad records continuous handwriting signals, which embody key characteristics of different people's handwriting habits, including position, speed, and acceleration. They use wavelet packet decomposition to process handwritten signals and extract the energy features of sub-bands, and the dimensionality of the dataset is decreased

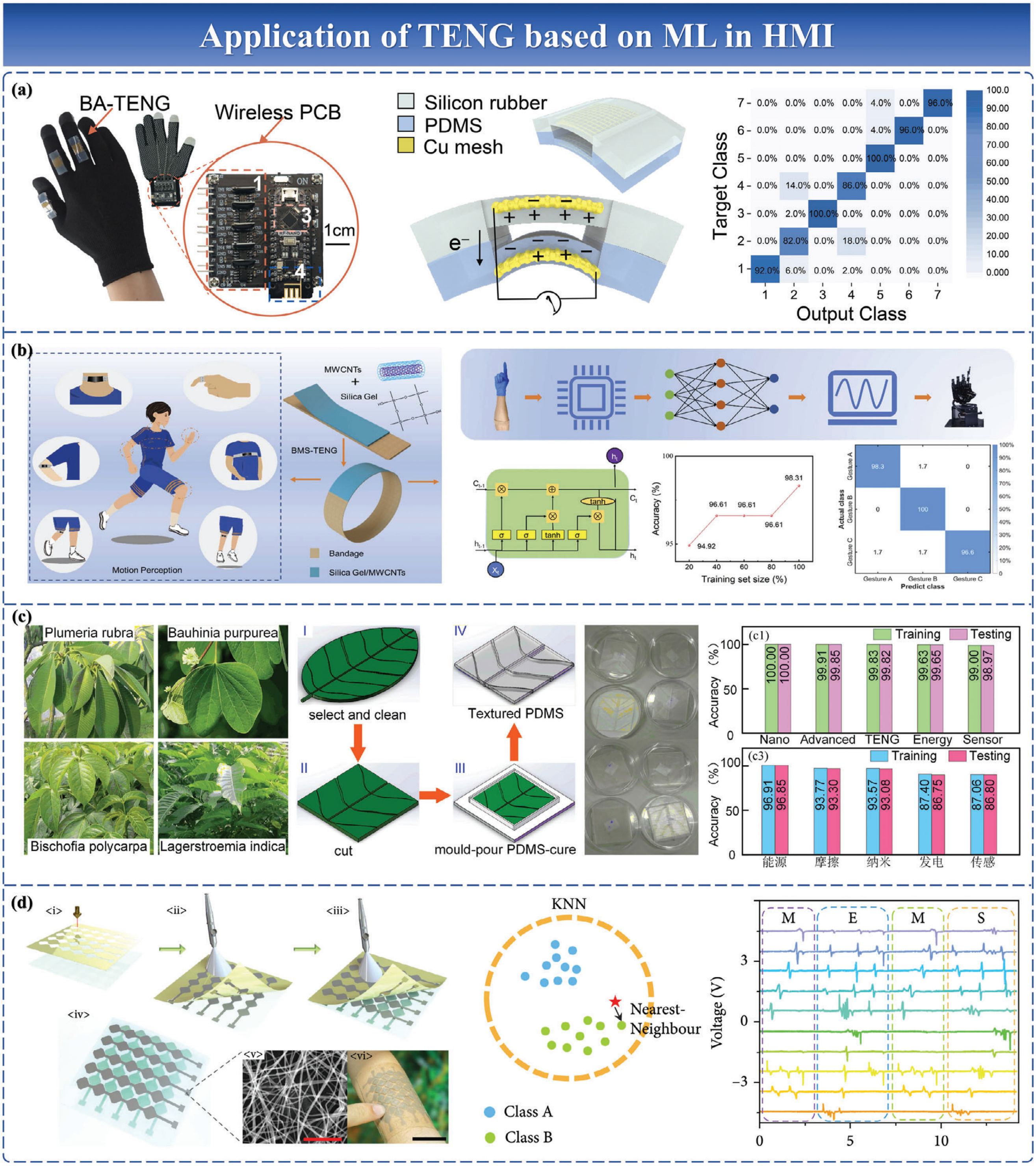

Figure 11. TENG-ML applications in HMI: a) The structure and working principle of BA-TENG, and the gesture recognition accuracy.[109] Copyright 2021, Elsevier. b) The schematic diagram and structure of BMS-TENG, and the process and accuracy of gesture recognition.[150] Copyright 2023, Elsevier. c) Structure and recognition accuracy of leaf-inspired TENG handwriting tablet.[157] Copyright 2020, Elsevier. d) The production process, structure, and object of symmetrical-array-electrode TENG, and the recognition accuracy of handwritten letters based on KNN algorithm.[159] Copyright 2021, Elsevier.

by PCA method. SVM and DT are used to recognize handwritten notes. Figure 10c shows that the classification accuracy of English words is the highest, exceeding 99%, while the Chinese characters are 91.36%, indicating that this method can effectively recognize handwriting written by different people. Ji et al. combined PDMS with braided copper mesh to fabricate highly sensitive flexible TENG for handwriting signal recognition.[113] They collect the handwriting signals of 26 letters to establish a fingerprint database of letters, and carry out feature recognition with Medium Gaussian SVM, with an accuracy of 93.5%. Lu et al. used digital infrared laser direct writing technology to fabricate interfinger electrodes, creating fingerprint-like microstructure on the packaging PDMS.[158] ML is used to recognize the signal differences of fingers sliding in 4 different directions on the surface of the device, achieving handwriting recognition to recognize character. Furthermore, they use a 1D-CNN model to automatically learn and classify 10 Braille digits after data collection, achieving a classification accuracy of 96.12%. Guo et al. designed a horizontal and vertical symmetrical array electrode structure with 25-pixel recognition capability, combining TENG and KNN to realize the classification of handwritten characters.[159] The object will pass through multiple electrode nodes when sliding on the TENG, and the trajectory of finger movement can be inferred by the number and order of signal peaks on the electrode. Therefore, the device can be used to recognize handwritten English letters, and each letter trace can produce a special triboelectric signal sequence (Figure 11d). They use PCA-KNN to label the handwriting triboelectric signals of different people after dimensionality reduction. English letters and user identities can be recognized simultaneously since different people have different writing habits. Yang et al. developed a TENG-based touchpad system by two channels to achieve signal recognition for 18 sliding modes.[160] 1D-CNN is optimized to recognize handwritten digital signals collected by a touchpad with 99.0% accuracy.

Touch is one of the most significant ways to comprehend surroundings. Meanwhile, tactile sensing plays a key role in smart sensing and control. Xing et al. proposed a double-shielded triboelectric tactile sensor with patterned flower-shaped holes for surface texture detection.[161] The measured object surface can generate signal output by rubbing the flower-shaped hole with the triboelectric layer. CNN is used to identify the surface texture of seven types of objects, and the recognition accuracy is up to 96.03%. Chun et al. fabricated a self-powered flexible neurotactile sensor to detect pressure distribution, and the TENG layered on the array to detect high-frequency vibrations.[162] By introducing micro-line patterns to simulate the functional properties of fingerprints, The device is able to classify 12 kinds of fabrics with complex patterns, and the recognition accuracy is 99.1%. Wei et al. used eggshell membrane and penetration method to construct a hybrid electronic skin with TENG and piezoresistive sensor in series to effectively perceive static and dynamic tactile information.[115] They innovatively import high-speed data collectors based on FPGA and multi-layer perceptron neural networks. Material properties are recognized in real time when touching smooth surface objects, demonstrating an exceptional ability to surpass human skin perception. Hou et al. fabricated a TENG-based embedded touch sensing system for real-time surface recognition for space robots.[163] The recognition surface can be divided into two categories, one is the space surface simulation material, such as Polyimide (PI) coating, and the other is the daily contact surface, such as sponge cushion. By dividing the recognition surface into several DT algorithms, all surfaces can be recognized with high precision. Wei et al. developed a smart sensing system using triboelectric triple tactile sensor array (TTS) to obtain properties belonging to each unknown material.[122] The TTS array consists of individual sensing units that respond in different order and peaks when exposed to different materials (**Figure 12a**). they developed a material recognition system utilizing images to extract feature points based on VGG model. TTS is integrated on the robotic arm for touch operation in the open environment, and the signals form a complete image that is fed into the VGG model, enabling accurate and real-time material recognition (96.62%).

In addition to simple tactile sensing and object recognition, TENG-ML can also be applied to digital twins, VR, and AR at a higher level to achieve deeper integration and application with artificial intelligence. Sun et al. fabricated low-cost triboelectric intelligent socks based on nitrile film, patterned silicone rubber film, and conductive textiles.[164] They use the smart sock as a controller for VR games. User moving will lead the sock to generate triboelectric signals, and then the entire spectrum data is wirelessly transmitted to the terminal. According to the received spectrum, CNN is selected to identify corresponding actions of the signals, and then the corresponding motion command is sent to Unity. In the demonstrated VR fitness game, the trained 1D-CNN can recognize human activities, including jumping, running, sliding, jumping, and walking, with a high accuracy of 96.7%. Unity can receive the recognized motion commands and convert them into virtual characters' motion. Zhu et al. proposed an ML-enhanced TENG for motion detection and virtual reality.[165] They use the CVD process to coat Cu electrode on patterned PTFE, and identify the vertical slide, L-shaped slide, Z-shaped slide on the PTFE through ML. It is found that PCA-K-means shows clearer clustering and visualization (99.13%) compared to t-SNE-K-means (97.10%). Characters in the virtual game can be controlled for specific movements by sliding vertically, L-shaped, and Z-shaped on the TENG.

Zhu et al. used 3D printing technology to fabricate TENG consisting of PTFE, Nylon for gait monitoring applications in virtual games.[135] The peak search algorithm is selected to detect the extreme point exceeding threshold. One sensing signal represents one action control in the virtual game. Therefore, as the human body takes a step, the character in the game takes a corresponding action. Jin et al. fabricated a TENG sensor, which is composed of a patterned electrode tactile sensor (T-TENG) and a geared structure length sensor (L-TENG) to enhance the smart application of soft manipulator.[166] L-TENG is used to control the bending motion of the robot finger, and T-TENG is used to change the bending direction. They combine TENG with SVM algorithm, and directly use the original voltage data in the 6-channel time domain as the sample characteristics, including contact force, speed, contact position, *etc.* Multi-classification SVM is used to classify the captured objects, and Figure 12b shows that the total recognition accuracy of the trained model reaches 97.1%. The manipulator system is applied to unmanned warehouses, which can achieve real-time monitoring and automatic sorting without the help of cameras. The identification results in real space can be projected into virtual space

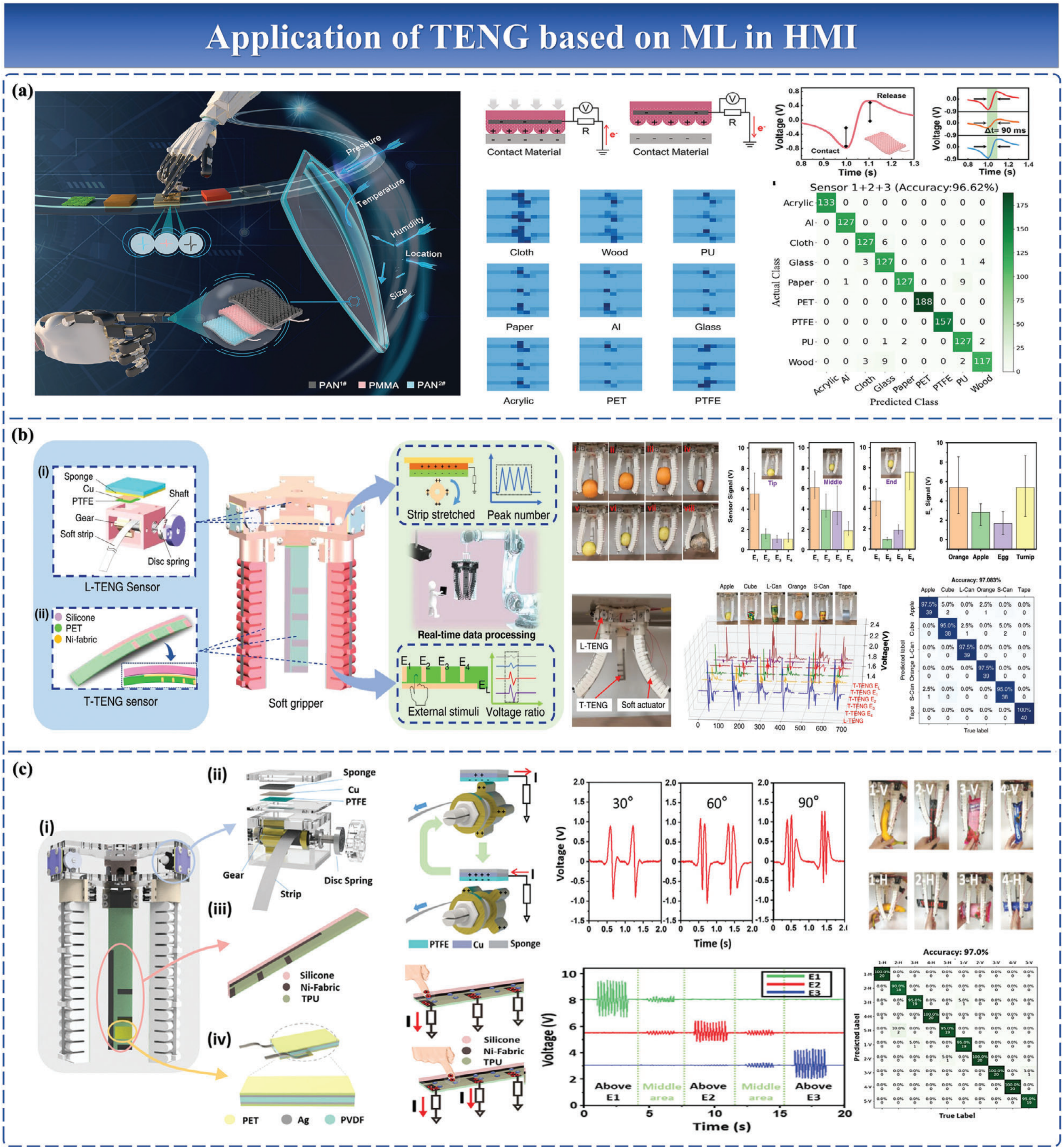

Figure 12. The multi-scenario application of TENG based on different algorithms: a) Schematic diagram, working principle, and recognition accuracy of material recognition sensor.[122] Copyright 2022, Wiley-VCH. b) Schematic diagram, principle, and recognition accuracy of TENG-based smart gripper.[166] Copyright 2020, Springer Nature. c) The structure, working principle, signal feature, and recognition accuracy of TENG-based smart gripper with sensing temperature.[167] Copyright 2021, Wiley-VCH.

in real time, demonstrating its potential in digital twin applications.

Furthermore, Sun et al. added a PVDF sensor to detect the temperature of the captured object on the basis of the above research.[167] Three-layer 1D-CNNs are constructed for feature extraction and automatic identification, and the accuracy of 28 objects with different shapes can reach 97.14% (Figure 12c). As the PVDF temperature detection channel is introduced, the recognition accuracy can reach almost 100%. The virtual store is successfully realized based on the improvement of the soft manipulator. The AIoT platform can synchronize the virtual operation of the user in the VR space and the execution of the robot arm in the real space, and provide accurate product feedback information through the high object identification precision of the robot hand, providing a more immersive online shopping experience.

In the future, the integration of TENG and ML will bring a more advanced environment for humans. By optimizing TENG to have more excellent characteristics, such as low cost, highly sensitive, ultra-stable and durable, and selecting the appropriate ML algorithm, a new era of artificial intelligence IoT will be built for every field.

6. Summary and Perspective

TENG has a diverse structure and stable output, while ML algorithm has strong data processing ability. The development of intelligent sensing systems based on TENG and ML has played a key role in driving the new era of IoT. Firstly, the combination of TENG and Bayes, RF, SVM, CNN, and RNN algorithms is introduced from the perspective of algorithm, which provides a reference for TENG to choose the appropriate algorithm in different situations. In addition, we present the application research status of TENG integrated with ML in the fields of health monitoring, fault detection, and HMI. The intelligent system built by ML-assisted TENG provides a more spacious direction and platform for the innovation of IoT technology, especially the part intersecting with artificial intelligence.

However, despite the increasing maturity of TENG and ML technology, there are still challenges that need to be solved in practice, which included the TENG, ML, and their integration:

1) It is difficult for TENG to recognize disorder stimuli, and the generated signals are susceptible to noise. Besides, there are still challenges in the bio-friendliness, corrosion resistance, and environmental harmfulness of the TENG. It is also difficult for TENG sensor to accurately perceive environmental parameters such as temperature, light, and humidity. In order to solve these problems, the TENG needs to be further optimized from the following aspects in the future.
   i) Material modification (physical or chemical modification), device design, environmental control, charge injection mechanism, and other methods can be used to improve the sensitivity and signal-to-noise ratio of TENG sensor. The physical modification mainly includes nanostructure, electrospinning, and nanoparticle filling, etc. The output performance is improved by increasing the surface contact area and dielectric constant of the triboelectric material. The chemical modification mainly includes surface functionalization, ion implantation, and chemical doping, which modifies the molecular characteristics of the material to improve the output performance. In addition, auxiliary techniques such as charge pump and power management can also effectively improve the signal-to-noise ratio and sensitivity of the TENG. In the future, the above methods can be used as the new strategy to improve the sensing of TENG effectively.
   ii) Excellent packaging technologies can also be used to encapsulate the TENG sensor, so as to enhance the stability of TENG sensor and reduce the implication of noise. In addition, the non-contact structure can effectively avoid heat loss and abrasion in friction, which greatly enhances the durability of TENG sensors. Methods to make full use of the non-contact structure and improve performance will be one of the major opportunities and challenges for the evolution of TENG sensors in the future.
   iii) It is necessary to choose appropriate materials, such as PDMS, FEP, and ECOFLEX, that consider flexibility, durability, and bio-friendliness. Temperature- and humidity-sensitive materials can also be selected into TENG to make the sensor temperature/humidity sensitive. Apart from commonly used polymers, there are numerous materials exhibiting excellent performance that can serve as valuable references for future material selection. Materials, such as biopolymer cellulose and chitosan, are not only environmentally friendly and recyclable, but also easy to be modified, thereby improving the signal-to-noise ratio and sensitivity of TENG sensor. In addition, inorganic materials are more resistant to temperature, humidity, and high pressure than polymers, such as graphene and other materials, providing new ideas for improving the stability of TENG. Finally, composite materials can combine the advantages of polymer and inorganic materials, such as MOFs,[168] taking into account the functional properties and mechanical properties of the component materials, which have excellent potential and will be a reliable choice of materials for TENG in the future.
2) ML is difficult to recognize amounts of features within a single time, and there are limitations to its mobility. It is difficult for ML to make the best decision when the application scenario changes dramatically. In addition, ML may have computational errors, data processing mismatches, time consuming, and overfitting problems. To solve related problems of ML with the application, future development should focus on the following aspects:
   i) First, for problems of excessive data computation and processing mismatch in ML, Batch Normalization can be used to amend the data set to meet the needs of TENG sensors for massive data processing. Besides, PCA can be used to map the original data to the new coordinate system, and find principal components in the data to reduce model complexity and avoid overfitting.[169] Meanwhile, t-SNE is the nonlinear dimensionality reduction algorithm that can calculate the similarity between data points in high-dimensional space and convert them into a probability distribution in low-dimensional spaces.[170] In addition, deep learning is a cutting-edge approach in ML, capable of learning more abstract, higher-level features and dealing with more complex problems. Therefore, optimizing the performance of deep learning algorithms in small sample models will be the future evolution trend of TENG sensors with the solving algorithm. Besides, deep learning is the advanced method in ML, which can effectively extract higher-level features and handle more complex problems. Therefore, optimizing their performance in small sample models will be the future development trend for the combination of TENG sensors and algorithms.

ii) In addition, in view of the problem of overfitting, methods such as random cropping and translation flipping can be used to expand the dataset, and Dropout and L_1/L_2 regularization can be selected to the algorithm model to prevent the weight of some nodes from being too large and reduce the occurrence of over-fitting. In addition, designing a more specific algorithm structure and selecting better activation functions and optimizers also are important research directions.

iii) Finally, aiming at the high cost of manual labeling of TENG output signals and the difficulty of data set construction, unsupervised learning, which is a learning method to learn the patterns in the original data without the help of labels, provides a new idea for solving this problem. Therefore, developing the novel unsupervised learning algorithm to fully extract and apply the features of TENG signals without adding manual annotation will become a major research content in the future.

3) The signals generated by TENG are one-dimensional signals that change with time series, and have fewer features than multidimensional data, thus affecting the recognition and judgment function. Meanwhile, in the process of recognition from the output of TENG to ML, there are multiple modules working together, including all kinds of circuits, such as rectifier current, buck circuit, etc., which makes the system too complicated and bloated, limiting its flexibility. In addition, the process of the system cannot really realize the concept of "real-time", it takes a long time from the data collection to identification, limiting the real large-scale commercial use. Cross-disciplinary research will be conducted in the following directions.

i) In order to solve the feature extraction problems, TENG-ML should further emphasize the all-round acquisition of signal characteristics in the future. The signal from TENG can be used as the image format, one-dimensional sequence signal can be converted into two-dimensional image data, and more details in TENG signal can be extracted by using CNN and other algorithms.

ii) Ensemble algorithms will become the future development trend, such as the combination of CNN and RNN. GRU units belonging to RNN algorithm can be applied to the CNN model, which not only extracted TENG signals as two-dimensional features of the image, but also combined the features under one-dimensional time series to further improve the recognition ability and accuracy of ML for TENG signals.

iii) In view of the low integration degree problem, the overall process framework can be considered optimized. The improvement of TENG's own characteristic and ML algorithm recognition ability can simplify the intermediate circuit processing module, which will be one of the alternative innovation directions in the future. Besides, chip technology has made rapid progress, which is expected to solve the above problems, and it is an important development direction in the future. Therefore, the TENG's signal acquisition, circuit processing, ML recognition, and other units can be integrated into the high-performance AI chip, which has the high-speed real-time calculation and discrimination, will achieve a truly highly integrated TENG-ML intelligent perception system. It is obvious that highly integrated TENG-ML intelligent systems will be a far-important research hotspot in the future.

In summary, the deep integration of TENG and ML is an important research content, which is expected to set off a new round of technological revolution in the field of IoT, especially in the direction of artificial intelligence. Therefore, TENG-ML has a very broad application prospect in the fields of HMI, intelligent sensing, and signal monitoring. In order to affect human daily life more deeply and achieve the future vision of "Internet of everything", TENG-ML should further develop in the direction of embedded highly integrated intelligent chip units, so as to pioneering deeper exploration in Intelligent Robots, Digital Twins, VR/AR, and other fields, and promote Intelligent Robots and the Digital World to truly enter People's Daily life.

Acknowledgements

This work was supported by the National key research and development program (2021YFB3203202), Beijing Municipal Natural Science Foundation (4232074 and 4122058), Fundamental Research Funds for the Central Universities (2020JBZD011), Talent Fund of Beijing Jiaotong University (2023XKRC034), National key research and development program (2021YFB3203200), National Natural Science Foundation of China (60706031 and 61574015), China National Postdoctoral Program for Innovative Talents (BX20230037), and China Postdoctoral Science Foundation (2023M730205).

Conflict of Interest

The authors declare no conflict of interest.

Author Contributions

J.Y. and K.H. contributed equally to this work. J.Y. prepared the manuscript. J.Y. and K.H. researched the literature on TENG and Machine Learning. J.Y. classified and analyzed the advanced literature. Y.H. and X.Z. checked the content of the manuscript. X.L., C.Z., and Z.W. reviewed and evaluated the manuscript and suggested revisions. Y.Q., W.S., and H.Z. proposed the supplementary content needed for the manuscript.

Keywords

Internet of Things, machine learning, self-powered sensing, triboelectric nanogenerator

Received: April 12, 2024
Revised: June 4, 2024
Published online:

[1] E. Hittinger, P. Jaramillo, *Science* **2019**, *364*, 326.
[2] J. M. Perkel, *Nature* **2017**, *542*, 125.
[3] I. McCulloch, M. Chabinyc, C. Brabec, C. B. Nielsen, S. E. Watkins, *Nat. Mater.* **2023**, *22*, 1304.
[4] S. Conti, G. Calabrese, K. Parvez, L. Pimpolari, F. Pieri, G. Iannaccone, C. Casiraghi, G. Fiori, *Nat. Rev. Mater.* **2023**, *8*, 651.

[5] G. Chen, X. Xiao, X. Zhao, T. Tat, M. Bick, J. Chen, *Chem. Rev.* **2022**, *122*, 3259.
[6] G. Chen, Y. Li, M. Bick, J. Chen, *Chem. Rev.* **2020**, *120*, 3668.
[7] N. Flores-Diaz, F. De Rossi, A. Das, M. Deepa, F. Brunetti, M. Freitag, *Chem. Rev.* **2023**, *123*, 9327.
[8] H. C. Ates, P. Q. Nguyen, L. Gonzalez-Macia, E. Morales-Narváez, F. Güder, J. J. Collins, C. Dincer, *Nat. Rev. Mater.* **2022**, *7*, 887.
[9] W. Tang, Q. Sun, Z. L. Wang, *Chem. Rev.* **2023**, *123*, 12105.
[10] P. Slade, M. J. Kochenderfer, S. L. Delp, S. H. Collins, *Nature* **2022**, *610*, 277.
[11] H. Du, S. Liu, F. You, J. Wang, Z. Ren, Z. Wu, *Prog. Nat. Sci.: Mater. Int.* **2021**, *31*, 557.
[12] K. Krishnamoorthy, P. Pazhamalai, S. Manoharan, N. U. H. Liyakath Ali, S. J. Kim, *Carbon Energy* **2022**, *4*, 833.
[13] X. Wu, Y. Guo, Y. Gu, F. Xie, M. Li, Z. Hu, H.-J. Lin, C.-W. Pao, Y.-C. Huang, C.-L. Dong, V. K. Peterson, R. Ran, W. Zhou, Z. Shao, *Carbon Energy* **2023**, *5*, e278.
[14] F. R. Fan, Z. Q. Tian, Z. Lin Wang, *Nano Energy* **2012**, *1*, 328.
[15] S. Dai, X. Li, C. Jiang, J. Ping, Y. Ying, *InfoMat* **2023**, *5*, e12391.
[16] X. Tao, X. Chen, Z. L. Wang, *Energy Environ. Sci.* **2023**, *16*, 3654.
[17] C. Zhang, Y. Hao, J. Yang, W. Su, H. Zhang, J. Wang, Z. L. Wang, X. Li, *Adv. Energy Mater.* **2023**, *13*, 2300387.
[18] M. Salauddin, S. M. S. Rana, M. Sharifuzzaman, H. S. Song, M. S. Reza, S. H. Jeong, J. Y. Park, *Adv. Energy Mater.* **2023**, *13*, 2203812.
[19] W. Lu, X. Q. Wang, C. Y. Wang, K. Gong, J. W. Li, X. Li, P. Wang, *Infomat* **2023**, e12508.
[20] Y. Z. Liu, S. Z. Yue, Z. Y. Tian, Z. J. Zhu, Y. J. Li, X. Y. Chen, Z. L. Wang, Z. Z. Yu, D. Yang, *Adv. Mater.* **2023**, 2309893.
[21] X. Pu, C. Zhang, Z. L. Wang, *Natl Sci Rev* **2022**, 10.
[22] C. Cao, Z. Li, F. Shen, Q. Zhang, Y. Gong, H. Guo, Y. Peng, Z. L. Wang, *Energy Environ. Sci.* **2024**, *17*, 885.
[23] P. I. P. Soares, J. P. Borges, *Prog. Nat. Sci.: Mater. Int.* **2021**, *31*, 835.
[24] Y. Hao, J. Yang, Z. Niu, M. Wang, H. Liu, Y. Qin, C. Zhang, X. Li, *Nano Energy* **2023**, *118*, 108964.
[25] Y. Song, J. Bao, Y. Hu, M. Xu, Z. Yang, Y. Liu, Q. Yang, C. Xiong, Z. Shi, *Nano Energy* **2022**, *103*, 107832.
[26] D. Yan, J. Ye, Y. Zhou, X. Lei, B. Deng, W. Xu, *Adv. Fiber Mater.* **2023**, *5*, 1852.
[27] S. Cho, K. Cha, B. Kim, J. Lee, K. Park, S. H. Chung, M. Song, D. Heo, J.-h. Son, M. Choi, Z. H. Lin, J. Hong, S. Lee, *Chem. Eng. J.* **2023**, *470*, 144283.
[28] S. Anwer, M. Umair Khan, B. Mohammad, Md. Rezeq, W. Cantwell, D. Gan, L. Zheng, *Chem. Eng. J.* **2023**, *470*, 144281.
[29] Y. Zheng, T. Liu, J. Wu, T. Xu, X. Wang, X. Han, H. Cui, X. Xu, C. Pan, X. Li, *Adv. Mater.* **2022**, *34*, 2202238.
[30] I. Mehamud, P. Marklund, M. Björling, Y. Shi, *Nano Energy* **2022**, *98*, 107292.
[31] Z. Li, B. Xu, J. Han, J. Huang, K. Y. Chung, *Adv. Energy Mater.* **2021**, *11*, 2101294.
[32] Q. Zhao, H. Wu, J. Wang, S. Xu, W. He, C. Shan, S. Fu, G. Li, K. Li, C. Hu, *Adv. Energy Mater.* **2023**, *13*, 2302099.
[33] N. Cui, C. Dai, J. Liu, L. Gu, R. Ge, T. Du, Z. Wang, Y. Qin, *Energy Environ. Sci.* **2020**, *13*, 2069.
[34] D. Lu, T. Liu, X. Meng, B. Luo, J. Yuan, Y. Liu, S. Zhang, C. Cai, C. Gao, J. Wang, S. Wang, S. Nie, *Adv. Mater.* **2023**, *35*, 2209117.
[35] S. Li, Z. Zhao, D. Liu, J. An, Y. Gao, L. Zhou, Y. Li, S. Cui, J. Wang, Z. L. Wang, *Adv. Mater.* **2022**, *34*, 2110363.
[36] P. Jiang, L. Zhang, H. Guo, C. Chen, C. Wu, S. Zhang, Z. L. Wang, *Adv. Mater.* **2019**, *31*, 1902793.
[37] H. Lin, Y. Liu, S. Chen, Q. Xu, S. Wang, T. Hu, P. Pan, Y. Wang, Y. Zhang, N. Li, Y. Li, Y. Ma, Y. Xie, L. Wang, *Nano Energy* **2019**, *65*, 103944.
[38] J. Hu, Y. Qian, F. Wei, J. Dai, D. Li, G. Zhang, H. Wang, W. Zhang, *Nano Energy* **2023**,.
[39] B. Xi, L. Wang, B. Yang, Y. Xia, D. Chen, X. Wang, *Nano Energy* **2023**, *110*, 108385.
[40] C. Chen, Z. Wen, J. Shi, X. Jian, P. Li, J. T. W. Yeow, X. Sun, *Nat. Commun.* **2020**, *11*, 4143.
[41] L. Xu, W. Xuan, J. Chen, C. Zhang, Y. Tang, X. Huang, W. Li, H. Jin, S. Dong, W. Yin, Y. Fu, J. Luo, *Nano Energy* **2021**, *83*, 105814.
[42] C. Cai, J. Mo, Y. Lu, N. Zhang, Z. Wu, S. Wang, S. Nie, *Nano Energy* **2021**, *83*, 105833.
[43] Y. Y. Ba, J. F. Bao, Z. Y. Wang, H. T. Deng, D. L. Wen, X. R. Zhang, C. Tu, X. S. Zhang, *Nano Energy* **2021**, *82*, 105730.
[44] P. Jiao, *Nano Energy* **2021**, *88*, 106227.
[45] C. Ning, K. Dong, R. Cheng, J. Yi, C. Ye, X. Peng, F. Sheng, Y. Jiang, Z. L. Wang, *Adv. Funct. Mater.* **2021**, *31*, 2006679.
[46] S. Ruiperez-Campillo, B. Deb, R. Feng, P. Ganesan, P. Clopton, A. Rogers, S. Narayan, *Europace* **2022**, 24.
[47] X. L. Wang, D. P. Yang, Y. S. Wang, H. Guo, N. N. Liu, W. W. Li, *Recent Res. Circuits, Syst., Mech. Transp. Syst., Proc. 10th WSEAS Int. Conf. Circuits, Syst., Electron., Control Signal Process. (CSECS '11), Proc. 7th WSEAS Int. Conf. Appl. Theor. Mech. (MECH. '11), Proc. 2nd Int. Conf. Automot. Transp. Syst. (ICAT '11)* **2020**, *139*, 106635.
[48] S. Ruiperez-Campillo, B. Deb, R. Feng, P. Ganesan, F. V. Y. Tjong, P. Clopton, A. J. Rogers, S. M. Narayan, *Eur. Heart J.* **2022**, 43.
[49] M. B. Schäfer, O. Zelenka, A. H. Nitz, H. Wang, S. Wu, Z. K. Guo, Z. Cao, Z. Ren, P. Nousi, N. Stergioulas, P. Iosif, A. E. Koloniari, A. Tefas, N. Passalis, F. Salemi, G. Vedovato, S. Klimenko, T. Mishra, B. Brügmann, E. Cuoco, E. A. Huerta, C. Messenger, F. Ohme, *Phys Rev D* **2023**, *107*, 023021.
[50] J. Chen, Z. Nie, F. Zhao, H. Jiang, L. Zhu, *Process Saf. Environ. Prot.* **2023**, *174*, 882.
[51] E. Ozer, J. Kufel, J. Myers, J. Biggs, G. Brown, A. Rana, A. Sou, C. Ramsdale, S. White, *Nat. Electron.* **2020**, *3*, 419.
[52] A. Sanchez-Aguilera, M. Masmudi-Martín, A. Navas-Olive, P. Baena, C. Hernández-Oliver, N. Priego, L. Cordón-Barris, L. Alvaro-Espinosa, S. García, S. Martínez, M. Lafarga, C. Sobrino, N. Ajenjo, M. J. Artiga, E. Ortega-Paino, V. García-Calvo, A. Pérez-Núñez, P. González-León, L. Jiménez-Roldán, L. M. Moreno, O. Esteban, J. M. Sepúlveda, O. Toldos, A. Hernández-Laín, A. Arenas, G. Blasco, J. F. Alén, A. d. l. L. Zaragoza, A. D. Núñez, L. Calero, et al., *Cancer Cell* **2023**, *41*, 1637.
[53] X. Yang, D. Chen, Q. Sun, Y. Wang, Y. Xia, J. Yang, C. Lin, X. Dang, Z. Cen, D. Liang, R. Wei, Z. Xu, G. Xi, G. Xue, C. Ye, L. P. Wang, P. Zou, S. Q. Wang, P. Rivera-Fuentes, S. Püntener, Z. Chen, Y. Liu, J. Zhang, Y. Zhao, *Cell Discov.* **2023**, *9*, 53.
[54] T. Mou, H. S. Pillai, S. Wang, M. Wan, X. Han, N. M. Schweitzer, F. Che, H. Xin, *Nat. Catal.* **2023**, *6*, 122.
[55] M. Li, L. Dai, Y. Hu, *ACS Energy Lett.* **2022**, *7*, 3204.
[56] S. M. Sohel Rana, M. Abu Zahed, M. Robiul Islam, O. Faruk, H. Su Song, S. Hoon Jeong, J. Yeong Park, *Chem. Eng. J.* **2023**, *473*, 144989.
[57] O. M. Katipoğlu, M. Sarıgöl, *Environ. Sci. Pollut. Res.* **2023**, *30*, 46074.
[58] C. Vişan, O. Pascu, M. Stănescu, E. D. Şandru, C. Diaconu, A. Buzo, G. Pelz, H. Cucu, *Knowledge-Based Systems* **2022**, *258*, 109987.
[59] M. Zare, M. Koch, *Neural Comput Appl* **2021**, *33*, 8067.
[60] D. Gao, R. Shenoy, S. Yi, J. Lee, M. Xu, Z. Rong, A. Deo, D. Nathan, J. G. Zheng, R. S. Williams, Y. Chen, *Adv. Mater.* **2023**, *35*, 2210484.
[61] F. Liu, Y. Feng, Y. Qi, G. Liu, H. Zhou, Y. Lin, B. Fan, Z. Zhang, S. Dong, C. Zhang, *InfoMat* **2023**, *5*, e12428.
[62] K. Sreeja Sadanandan, Z. Saadi, C. Murphy, I. Grikalaite, M. F. Craciun, A. I. S. Neves, *Nano Energy* **2023**, *116*, 108797.
[63] Z. Xu, D. Zhang, H. Cai, Y. Yang, H. Zhang, C. Du, *Nano Energy* **2022**, *102*, 107719.
[64] L. Long, W. Liu, Z. Wang, W. He, G. Li, Q. Tang, H. Guo, X. Pu, Y. Liu, C. Hu, *Nat. Commun.* **2021**, *12*, 4689.
[65] J. Jeong, S. Jeon, X. Ma, Y. W. Kwon, D. M. Shin, S. W. Hong, *Adv. Mater.* **2021**, *33*, 2102530.

[66] C. Zhang, Y. Liu, B. Zhang, O. Yang, W. Yuan, L. He, X. Wei, J. Wang, Z. L. Wang, *ACS Energy Lett.* **2021**, *6*, 1490.
[67] W. Akram, Q. Chen, G. Xia, J. Fang, *Nano Energy* **2023**, *106*, 108089.
[68] K. Munirathinam, D. S. Kim, A. Shanmugasundaram, J. Park, Y. J. Jeong, D. W. Lee, *Nano Energy* **2022**, *102*, 107675.
[69] S. Zhang, S. Meng, K. Zhang, Z. Wang, X. Xu, C. Zhi, S. Shi, J. Hu, *Nano Energy* **2023**, *112*, 108443.
[70] Z. Yang, Y. Yang, F. Liu, B. Li, Y. Li, X. Liu, J. Chen, C. Wang, L. Ji, Z. L. Wang, J. Cheng, *Nano Energy* **2022**, *98*, 107264.
[71] X. Li, T. H. Lau, D. Guan, Y. Zi, *J. Mater. Chem. A* **2019**, *7*, 19485.
[72] T. Wang, G. Gu, W. Shang, J. Gan, W. Zhang, H. Luo, B. Zhang, P. Cui, J. Guo, F. Yang, G. Cheng, Z. Du, *Nano Energy* **2021**, *90*, 106518.
[73] Y. Xi, J. Wang, Y. Zi, X. Li, C. Han, X. Cao, C. Hu, Z. Wang, *Nano Energy* **2017**, *38*, 101.
[74] Y. Yang, Y. Yang, J. Huang, S. Li, Z. Meng, W. Cai, Y. Lai, *Adv. Fiber Mater.* **2023**, *5*, 1505.
[75] T. X. Xiao, X. Liang, T. Jiang, L. Xu, J. J. Shao, J. H. Nie, Y. Bai, W. Zhong, Z. L. Wang, *Adv. Funct. Mater.* **2018**, *28*, 1802634.
[76] S. Hu, J. Weber, S. Chang, G. Xiao, J. Lu, J. Gao, W. Jiang, Y. Zhang, Y. Tao, *Adv. Mater. Technol.* **2022**, *7*, 2200186.
[77] H. Yang, M. Wang, M. Deng, H. Guo, W. Zhang, H. Yang, Y. Xi, X. Li, C. Hu, Z. Wang, *Nano Energy* **2019**, *56*, 300.
[78] Z. Yuan, X. Du, H. Niu, N. Li, G. Shen, C. Li, Z. L. Wang, *Nanoscale* **2019**, *11*, 495.
[79] H. Li, J. Wen, Z. Ou, E. Su, F. Xing, Y. Yang, Y. Sun, Z. L. Wang, B. Chen, *Adv. Funct. Mater.* **2023**, *33*, 2212207.
[80] J. Meng, L. Zhang, H. Liu, W. Sun, W. Wang, H. Wang, D. Yang, M. Feng, Y. Feng, D. Wang, *Adv. Energy Mater. n/a*, 2303298.
[81] S. W. Chen, X. Cao, N. Wang, L. Ma, H. R. Zhu, M. Willander, Y. Jie, Z. L. Wang, *Adv. Energy Mater.* **2017**, *7*, 1601255.
[82] H. Wu, Z. Wang, B. Zhu, H. Wang, C. Lu, M. Kang, S. Kang, W. Ding, L. Yang, R. Liao, J. Wang, Z. L. Wang, *Adv. Energy Mater.* **2023**, *13*, 2300051.
[83] L. Jin, S. L. Zhang, S. Xu, H. Guo, W. Yang, Z. L. Wang, *Adv. Mater. Technol.* **2021**, *6*, 2000918.
[84] Z. Lin, B. Zhang, H. Guo, Z. Wu, H. Zou, J. Yang, Z. L. Wang, *Nano Energy* **2019**, *64*, 103908.
[85] Y. Xi, H. Guo, Y. Zi, X. Li, J. Wang, J. Deng, S. Li, C. Hu, X. Cao, Z. L. Wang, *Adv. Energy Mater.* **2017**, *7*, 1602397.
[86] M. Stern, D. Hexner, J. W. Rocks, A. J. Liu, *Phys. Rev. X* **2021**, *11*, 021045.
[87] I. Walsh, D. Fishman, D. Garcia-Gasulla, T. Titma, G. Pollastri, E. Capriotti, R. Casadio, S. Capella-Gutierrez, D. Cirillo, A. Del Conte, A. C. Dimopoulos, V. D. Del Angel, J. Dopazo, P. Fariselli, J. M. Fernández, F. Huber, A. Kreshuk, T. Lenaerts, P. L. Martelli, A. Navarro, P. Ó. Broin, J. Piñero, D. Piovesan, M. Reczko, F. Ronzano, V. Satagopam, C. Savojardo, V. Spiwok, M. A. Tangaro, G. Tartari, et al., *Nat. Methods* **2021**, *18*, 1122.
[88] L. Zaadnoordijk, T. R. Besold, R. Cusack, *Nature Machine Intelligence* **2022**, *4*, 510.
[89] R. Patel, N. Jayatilleke, R. Jackson, R. Stewart, P. McGuire, *Lancet* **2014**, *383*, S16.
[90] J. Tolles, W. J. Meurer, *JAMA, J. Am. Med. Assoc.* **2016**, *316*, 533.
[91] E. Audureau, P. L. Soubeyran, C. Martinez-Tapia, C. A. Bellera, S. Bastuji-Garin, P. Boudou-Rouquette, M. Rainfray, A. Chahwakilian, T. Grellety, O. Hanon, S. Mathoulin-Pélissier, E. Paillaud, F. Canoui-Poitrine, *J. Clin. Oncol.* **2019**, *37*, 11516.
[92] D. T. Ahneman, J. G. Estrada, S. Lin, S. D. Dreher, A. G. Doyle, *Science* **2018**, *360*, 186.
[93] H. Samet, *IEEE Trans Pattern Anal Mach Intell* **2008**, *30*, 243.
[94] N. Y. Yürüşen, B. Uzunoğlu, A. P. Talayero, A. L. Estopiñán, *Renewable Energy* **2021**, *175*, 702.
[95] W. S. Noble, *Nat. Biotechnol.* **2006**, *24*, 1565.
[96] M. Chen, U. Challita, W. Saad, C. Yin, M. Debbah, *IEEE Communications Surveys & Tutorials* **2019**, *21*, 3039.
[97] S. B. Jeon, Y. H. Nho, S. J. Park, W. G. Kim, I. W. Tcho, D. Kim, D. S. Kwon, Y. K. Choi, *Nano Energy* **2017**, *41*, 139.
[98] C. Zhang, L. Zhang, Y. Tian, B. Bao, D. Li, *Appl. Sci.* **2023**, *13*, 3885.
[99] Q. Han, Z. Jiang, X. Xu, Z. Ding, F. Chu, *Recent Res. Circuits, Syst., Mech. Transp. Syst., Proc. 10th WSEAS Int. Conf. Circuits, Syst., Electron., Control Signal Process. (CSECS '11), Proc. 7th WSEAS Int. Conf. Appl. Theor. Mech. (MECH. '11), Proc. 2nd Int. Conf. Automot. Transp. Syst. (ICAT '11)* **2022**, *166*, 108382.
[100] H. Luo, J. Du, P. Yang, Y. Shi, Z. Liu, D. Yang, L. Zheng, X. Chen, Z. L. Wang, *ACS Appl. Mater. Interfaces* **2023**, *15*, 17009.
[101] Q. Cheng, X. Jiang, H. Zhang, W. Wang, C. Sun, *Sustainability* **2020**, *12*, 8926.
[102] Y. Jiang, J. An, F. Liang, G. Zuo, J. Yi, C. Ning, H. Zhang, K. Dong, Z. L. Wang, *Nano Res.* **2022**, *15*, 8389.
[103] Y. Yang, X. Hou, W. Geng, J. Mu, L. Zhang, X. Wang, J. He, J. Xiong, X. Chou, *Sci. China Technol. Sci.* **2022**, *65*, 826.
[104] J. Yun, J. Park, S. Jeong, D. Hong, D. Kim, *Polymers* **2022**, *14*, 3549.
[105] J. N. Kim, J. Lee, H. Lee, I. K. Oh, *Nano Energy* **2021**, *82*, 105705.
[106] J. Liu, J. Chen, F. Dai, J. Zhao, S. Li, Y. Shi, W. Li, L. Geng, M. Ye, X. Chen, Y. Liu, W. Guo, *Nano Energy* **2022**, *103*, 107764.
[107] W. Zhang, P. Wang, K. Sun, C. Wang, D. Diao, *Nano Energy* **2019**, *56*, 277.
[108] D. Zhao, K. Zhang, Y. Meng, Z. Li, Y. Pi, Y. Shi, J. You, R. Wang, Z. Dai, B. Zhou, J. Zhong, *Nano Energy* **2022**, *100*, 107500.
[109] Y. Luo, Z. Wang, J. Wang, X. Xiao, Q. Li, W. Ding, H. Y. Fu, *Nano Energy* **2021**, *89*, 106330.
[110] P. Sun, N. Cai, X. Zhong, X. Zhao, L. Zhang, S. Jiang, *Nano Energy* **2021**, *89*, 106492.
[111] Y. Tong, Z. Feng, J. Kim, J. L. Robertson, X. Jia, B. N. Johnson, *Nano Energy* **2020**, *75*, 104973.
[112] H. Zhou, D. Li, X. He, X. Hui, H. Guo, C. Hu, X. Mu, Z. L. Wang, *Adv. Sci.* **2021**, *8*, 2101020.
[113] X. Ji, T. Zhao, X. Zhao, X. Lu, T. Li, *Adv. Mater. Technol.* **2020**, *5*, 1900921.
[114] N. Zhou, H. Ao, X. Chen, S. Gao, H. Jiang, *Nano Res.* **2023**, *16*, 10120.
[115] X. Wei, H. Li, W. Yue, S. Gao, Z. Chen, Y. Li, G. Shen, *Matter* **2022**, *5*, 1481.
[116] Q. Zhang, T. Jin, J. Cai, L. Xu, T. He, T. Wang, Y. Tian, L. Li, Y. Peng, C. Lee, *Adv. Sci.* **2022**, *9*, 2103694.
[117] H. Yao, Z. Wang, Y. Wu, Y. Zhang, K. Miao, M. Cui, T. Ao, J. Zhang, D. Ban, H. Zheng, *Adv. Funct. Mater.* **2022**, *32*, 2112155.
[118] M. Jiang, B. Li, W. Jia, Z. Zhu, *Nano Energy* **2022**, *93*, 106830.
[119] N. Li, Z. Yin, W. Zhang, C. Xing, T. Peng, B. Meng, J. Yang, Z. Peng, *Nano Energy* **2022**, *96*, 107102.
[120] F. Wen, Z. Sun, T. He, Q. Shi, M. Zhu, Z. Zhang, L. Li, T. Zhang, C. Lee, *Adv. Sci.* **2020**, *7*, 2000261.
[121] J. Zhu, Z. Sun, J. Xu, R. D. Walczak, J. A. Dziuban, C. Lee, *Sci. Bull.* **2021**, *66*, 1176.
[122] X. Wei, B. Wang, Z. Wu, Z. L. Wang, *Adv. Mater.* **2022**, *34*, 2203073.
[123] N. T. Beigh, F. Beigh, S. Naval, D. Mukherjee, D. Mallick, presented at *2023 IEEE 36th Int. Conf. on Micro Electro Mechanical Systems (MEMS)*, München, Germany, January **2023**.
[124] Z. Qin, Y. Wang, Z. Yuan, D. Yu, Z. Xie, *Sens. Actuators, A* **2023**, *359*, 114455.
[125] Y. Lu, H. Tian, J. Cheng, F. Zhu, B. Liu, S. Wei, L. Ji, Z. L. Wang, *Nat. Commun.* **2022**, *13*, 1401.
[126] C. Ye, S. Yang, J. Ren, S. Dong, L. Cao, Y. Pei, S. Ling, *ACS Nano* **2022**, *16*, 4415.
[127] R. Mao, D. Zhang, Z. Wang, H. Zhang, D. Wang, M. Tang, L. Zhou, H. Cai, H. Xia, *Nano Energy* **2023**, *111*, 108418.

[128] R. Xu, F. Luo, Z. Zhu, M. Li, B. Chen, *ACS Appl. Electron. Mater.* **2022**, *4*, 4051.
[129] Q. Zheng, Y. Hou, H. Yang, P. Tan, H. Shi, Z. Xu, Z. Ye, N. Chen, X. Qu, X. Han, Y. Zou, X. Cui, H. Yao, Y. Chen, W. Yao, J. Zhang, Y. Chen, J. Liang, X. Gu, D. Wang, Y. Wei, J. Xue, B. Jing, Z. Zeng, L. Wang, Z. Li, Z. L. Wang, *Nano Energy* **2022**, *98*, 107245.
[130] X. Ji, P. Fang, B. Xu, K. Xie, H. Yue, X. Luo, Z. Wang, X. Zhao, P. Shi, *Nano Lett.* **2020**, *20*, 4043.
[131] Z. Zhang, Q. Shi, T. He, X. Guo, B. Dong, J. Lee, C. Lee, *Nano Energy* **2021**, *90*, 106517.
[132] S. An, X. Pu, S. Zhou, Y. Wu, G. Li, P. Xing, Y. Zhang, C. Hu, *ACS Nano* **2022**, *16*, 9359.
[133] A. Babu, S. Ranpariya, D. K. Sinha, D. Mandal, *Adv. Mater. Technol.* **2023**, *8*, 2300046.
[134] G. Ye, Y. Wan, J. Wu, W. Zhuang, Z. Zhou, T. Jin, J. Zi, D. Zhang, X. Geng, P. Yang, *Nano Energy* **2022**, *97*, 107148.
[135] Y. Zhu, F. Sun, C. Jia, C. Huang, K. Wang, Y. Li, L. Chou, Y. Mao, *Sustainability* **2022**, *14*, 10875.
[136] J. Li, Z. Wang, Z. Zhao, Y. Jin, J. Yin, S. L. Huang, J. Wang, *UbiComp ISWC* **2021**, 643.
[137] L. Yang, Y. Wang, Z. Zhao, Y. Guo, S. Chen, W. Zhang, X. Guo, *ACS Appl. Mater. Interfaces* **2020**, *12*, 38192.
[138] J. Yu, Y. Wen, L. Yang, Z. Zhao, Y. Guo, X. Guo, *Nano Energy* **2022**, *92*, 106698.
[139] J. Zhu, M. Cho, Y. Li, T. He, J. Ahn, J. Park, T. L. Ren, C. Lee, I. Park, *Nano Energy* **2021**, *86*, 106035.
[140] D. Hasan, J. Zhu, H. Wang, O. B. Sulaiman, M. S. Yazici, T. Grzebyk, R. D. Walczak, J. A. Dziuban, C. Lee, presented at *2019 19th Int. Conf. on Micro and Nanotechnology for Power Generation and Energy Conversion Applications (PowerMEMS)*, Krakow, Poland, December **2019**.
[141] Q. Han, Z. Jiang, Y. Kong, F. Chu, *IEEE ASME Trans Mechatron* **2022**, *27*, 4686.
[142] F. Shen, Z. Li, C. Xin, H. Guo, Y. Peng, K. Li, *ACS Appl. Mater. Interfaces* **2022**, *14*, 3437.
[143] Y. Yang, J. Wang, J. Lou, H. Yao, C. Zhao, *Chem. Eng. J.* **2023**, *471*, 144582.
[144] S. Tkachev, M. Monteiro, J. Santos, E. Placidi, M. B. Hassine, P. Marques, P. Ferreira, P. Alpuim, A. Capasso, *Adv. Funct. Mater.* **2021**, *31*, 2103287.
[145] S. Cho, S. Kang, A. Pandya, R. Shanker, Z. Khan, Y. Lee, J. Park, S. L. Craig, H. Ko, *ACS Nano* **2017**, *11*, 4346.
[146] X. Li, P. Zhu, S. Zhang, X. Wang, X. Luo, Z. Leng, H. Zhou, Z. Pan, Y. Mao, *ACS Nano* **2022**, *16*, 5909.
[147] W. Ding, A. C. Wang, C. Wu, H. Guo, Z. L. Wang, *Adv. Mater. Technol.* **2019**, *4*, 1800487.
[148] S. Liang, C. Li, M. Niu, P. Zhu, Z. Pan, Y. Mao, *JPhys Mater.* **2024**, *7*, 012001.
[149] X. Ge, Z. Gao, L. Zhang, H. Ji, J. Yi, P. Jiang, Z. Li, L. Shen, X. Sun, Z. Wen, *Nano Energy* **2023**, *113*, 108541.
[150] C. Zheng, W. Li, Y. Shi, S. Wei, K. Liu, J. Cheng, L. Ji, Y. Lu, *Nano Energy* **2023**, *109*, 108245.
[151] F. Wen, T. He, Q. Shi, T. Zhang, C. Lee, *2020 IEEE 33rd International Conference on Micro Electro Mechanical Systems (MEMS)*, Vancouver, BC, January **2020**.
[152] M. H. Syu, Y. J. Guan, W. C. Lo, Y. K. Fuh, *Nano Energy* **2020**, *76*, 105029.
[153] J. Yang, S. Liu, Y. Meng, W. Xu, S. Liu, L. Jia, G. Chen, Y. Qin, M. Han, X. Li, *ACS Appl. Mater. Interfaces* **2022**, *14*, 25629.
[154] H. J. Yoon, D. H. Kim, W. Seung, U. Khan, T. Y. Kim, T. Kim, S. W. Kim, *Nano Energy* **2019**, *63*, 103857.
[155] X. Chen, J. Xiong, K. Parida, M. Guo, C. Wang, C. Wang, X. Li, J. Shao, P. S. Lee, *Nano Energy* **2019**, *64*, 103904.
[156] S. Chun, C. Pang, S. B. Cho, *Adv. Mater.* **2020**, *32*, 1905539.
[157] W. Zhang, L. Deng, L. Yang, P. Yang, D. Diao, P. Wang, Z. L. Wang, *Nano Energy* **2020**, *77*, 105174.
[158] Y. Lu, D. Kong, G. Yang, R. Wang, G. Pang, H. Luo, H. Yang, K. Xu, *Adv. Sci.* **2023**, *10*, 2303949.
[159] H. Guo, J. Wan, H. Wang, H. Wu, C. Xu, L. Miao, M. Han, H. Zhang, *Research* **2021**, 2021.
[160] X. Yang, J. Yin, Z. Wang, Z. Song, J. Song, W. Ding, *UbiComp ISWC* **2021**, 697.
[161] P. Xing, S. An, Y. Wu, G. Li, S. Liu, J. Wang, Y. Cheng, Y. Zhang, X. Pu, *Nano Energy* **2023**, *116*, 108758.
[162] S. Chun, W. Son, H. Kim, S. K. Lim, C. Pang, C. Choi, *Nano Lett.* **2019**, *19*, 3305.
[163] X. Hou, L. Zhang, Y. Su, G. Gao, Y. Liu, Z. Na, Q. Xu, T. Ding, L. Xiao, L. Li, T. Chen, *Nano Energy* **2023**, *105*, 108013.
[164] Z. Zhang, T. He, M. Zhu, Z. Sun, Q. Shi, J. Zhu, B. Dong, M. R. Yuce, C. Lee, *npj Flexible Electron.* **2020**, *4*, 29.
[165] J. Zhu, S. Ji, J. Yu, H. Shao, H. Wen, H. Zhang, Z. Xia, Z. Zhang, C. Lee, *Nano Energy* **2022**, *103*, 107766.
[166] T. Jin, Z. Sun, L. Li, Q. Zhang, M. Zhu, Z. Zhang, G. Yuan, T. Chen, Y. Tian, X. Hou, C. Lee, *Nat. Commun.* **2020**, *11*, 5381.
[167] Z. Sun, M. Zhu, Z. Zhang, Z. Chen, Q. Shi, X. Shan, R. C. H. Yeow, C. Lee, *Adv. Sci.* **2021**, *8*, 2100230.
[168] G. Khandelwal, A. Chandrasekhar, N. P. Maria Joseph Raj, S. J. Kim, *Adv. Energy Mater.* **2019**, *9*, 1803581.
[169] S. X. Wu, H. T. Wai, L. Li, A. Scaglione, *Proc IEEE Inst Electr Electron Eng* **2018**, *106*, 1321.
[170] W. Lu, X. Yan, *ISA Trans* **2022**, *122*, 163.

Jiayi Yang is currently pursuing his Ph.D. degree under Prof. Xiuhan Li at Beijing Jiaotong University, Beijing, China. His current research mainly centers on self-powered wearable sensors with triboelectric nanogenerator for artificial intelligent sensing system.

Keke Hong is currently a Master's student under the supervision of Prof. Xiuhan Li at Beijing Jiaotong University, Beijing, China. Her current research mainly focuses on triboelectric nanogenerators and machine learning.

Yijun Hao is currently pursuing his Ph.D. degree under Prof. Xiuhan Li at Beijing Jiaotong University, Beijing, China. His current research mainly centers on self-powered wearable device and Internet of Things systems, which are based on triboelectric nanogenerators.

Xiaopeng Zhu is currently a doctoral student under the supervision of Prof. Xiuhan Li at Beijing Jiaotong University, Beijing, China. His research focuses on the design and fabrication of charge-excitation triboelectric nanogenerators.

Yong Qin is the vice dean of State Key Laboratory of Rail Traffic Control and Safety, Beijing Jiaotong University. He received his Ph.D. degree from China Academy of Railway Sciences in Information Engineering and Control in 1999. His research area mainly focused on prognostics and health management for rail transportation system, transit network safety and reliability, rail operation planning and optimization, and intelligent transportation system. He has authored or coauthored more than 100 publication papers (SCI/EI), one ESI highly cited paper, five Chinese books, and two English books, and has 23 patents granted including two USA patents.

Wei Su is a professor at Beijing Jiaotong University, and deputy director of the National Engineering Research Center for Mobile Private Networks. He received his Ph.D. degree from Beijing Jiaotong University in 2008. He is mainly engaged in the research of new generation information network theory and key technologies, mobile Internet theory and key technologies.

Hongke Zhang is a professor at Beijing Jiaotong University and the director of the National Engineering Research Center for Mobile Private Networks. He received his Ph.D. degree from the University of Electronic Science and Technology in 1993. He is engaged in the research of private communication network theory and engineering technology, and has established the functional structure of identification network and the analytical mapping mechanism, effectively solving the problems of high mobile support and high reliable transmission in complex scenarios.

Chuguo Zhang received his Ph.D. degree from the University of Chinese Academy of Sciences in 2022. Currently, he is an associate professor at Beijing Jiaotong University. His current research interests focus on the design and research of passive node system in Internet of Things system, which is based on triboelectric nanogenerator.

Zhong Lin Wang received his Ph.D. from Arizona State University in physics. He is the director of Beijing Institute of Nanoenergy and Nanosystems. Prof. Wang has made original and innovative contributions to the fundamental physical properties of oxide nanobelts and nanowires. His discoveries and breakthroughs in the development of nanogenerators established the principles and technical roadmap for harvesting mechanical energy from environmental and biological systems to power electronics. His research on self-powered nano-systems has inspired worldwide academic and industry efforts in energy research on micro-nanosystems, which are now a unique discipline for energy research and future sensor networks.

Xiuhan Li is currently a professor at the School of Electronics and Information Engineering, Beijing Jiaotong University. She received her Ph.D. degree in microelectronics and solid state electronics from the Peking University in 2006. Her research interests mainly focused on Micro/nano devices and energy harvesting, implantable biomedical microdevices especially for wireless energy transfer system. She has directed and participated in a number of projects from Ministry of Science and Technology and NSFC. Prof. Li has published more than 30 peer-reviewed papers (Adv. Mater., ACS Nano, Nano Energy, etc.) and authorized six invention patents.